J. Fluid Mech. (1995), *vol.* 299, *pp.* 153–186

Magnetic damping of jets and vortices

By P. A. DAVIDSON

Department of Engineering, University of Cambridge, Trumpington Street, Cambridge CB2 1PZ, UK

(Received 20 September 1994 and in revised form 22 May 1995)

It is well known that the imposition of a static magnetic field tends to suppress motion in an electrically conducting liquid. Here we look at the magnetic damping of liquid-metal flows where the Reynolds number is large and the magnetic Reynolds number is small. The magnetic field is taken as uniform and the fluid is either infinite in extent or else bounded by an electrically insulating surface S. Under these conditions, we find that three general principles govern the flow. First, the Lorentz force destroys kinetic energy but does not alter the net linear momentum of the fluid, nor does it change the component of angular momentum parallel to $\boldsymbol{B}$. In certain flows, this implies that momentum, linear or angular, is conserved. Second, the Lorentz force guides the flow in such a way that the global Joule dissipation, D, decreases, and this decline in D is even more rapid than the corresponding fall in global kinetic energy, E. (Note that both D and E are quadratic in $\boldsymbol{u}$.) Third, this decline in relative dissipation, D/E, is essential to conserving momentum, and is achieved by propagating linear or angular momentum out along the magnetic field lines. In fact, this spreading of momentum along the $\boldsymbol{B}$-lines is a diffusive process, familiar in the context of MHD turbulence. We illustrate these three principles with the aid of a number of specific examples. In increasing order of complexity we look at a spatially uniform jet evolving in time, a three-dimensional jet evolving in space, and an axisymmetric vortex evolving in both space and time. We start with a spatially uniform jet which is dissipated by the sudden application of a transverse magnetic field. This simple (perhaps even trivial) example provides a clear illustration of our three general principles. It also provides a useful stepping-stone to our second example of a steady three-dimensional jet evolving in space. Unlike the two-dimensional jets studied by previous investigators, a three-dimensional jet cannot be annihilated by magnetic braking. Rather, its cross-section deforms in such a way that the momentum flux of the jet is conserved, despite a continual decline in its energy flux. We conclude with a discussion of magnetic damping of axisymmetric vortices. As with the jet flows, the Lorentz force cannot destroy the motion, but rather rearranges the angular momentum of the flow so as to reduce the global kinetic energy. This process ceases, and the flow reaches a steady state, only when the angular momentum is uniform in the direction of the field lines. This is closely related to the tendency of magnetic fields to promote two-dimensional turbulence.

1. Introduction

It is well known that a static magnetic field can suppress motion in an electrically conducting liquid. To some extent, the mechanism is clear. Motion of the liquid across the magnetic field lines induces a current. This leads to Joule dissipation and the resulting rise in thermal energy is accompanied by a corresponding fall in kinetic energy. It is as if each element of fluid experiences a frictional drag. Indeed, the concept

of a frictional force is not a bad one in two-dimensional flows where, as we shall see, the Lorentz force is of the form $-\tau^{-1}\boldsymbol{u}_\perp$, where τ is a time constant related to the applied magnetic field and $\boldsymbol{u}_\perp$ represents the velocity components perpendicular to the field lines.

In recent years this phenomenon has been exploited in a range of metallurgical processes, as well as in the laboratory. For example, in the continuous casting of steel, a static magnetic field is often used to suppress motion within the mould. Sometimes this motion takes the form of a submerged jet, which feeds the mould from above, and sometimes it takes the form of large eddies or vortices (Szekeley *et al.* 1992). In other solidification processes, such as the continuous casting of aluminium, or the Bridgeman technique for growing semiconductor crystals, it is widely believed that natural convection has a detrimental effect on the structure of the final product (Davidson & Flood 1994). As in the casting of steel, the imposition of a static magnetic field is seen as one means of suppressing these unwanted motions. (See, for example, Alboussiere, Garandet & Moreau 1993, and Muller, Neumann & Weber 1984.)

Magnetic damping is also employed in the laboratory. An early example is the use of a static magnetic field to delay the onset of Rayleigh–Bénard convection in a fluid heated from below. (See, for example, Moreau 1990.) A more recent example arises in the 'hot-wire' technique for measuring the thermal conductivity of liquid metals. Here the conductivity is determined by monitoring the rate at which heat diffuses into the liquid from a long thin vertical wire. This technique relies on conduction being dominant over convection. Yet natural convection is always present to some degree in the form of an axisymmetric buoyant plume (Saito, Matsumoto & Utaka 1987). Again, magnetic damping is one means of suppressing the unwanted motion (Nakamura *et al.* 1990). This is illustrated in figure 1(*a*).

Clearly, there are a number of important commercial processes where a static magnetic field is used to suppress unwanted motion. Frequently these flows take the form of submerged jets or eddies, and often they are driven by buoyancy. In this paper we consider the influence of a uniform magnetic field on both submerged jets and isolated vortices (see figure 1). We shall include buoyancy, but only to the extent that it may be used to maintain a vertical jet (figure 1*a*).

This study touches on two traditional fields of research. One is the damping of turbulent flows by a static magnetic field. The other is the suppression of submerged jets by magnetic damping. We shall postpone our review of MHD turbulence until §3.2, as it requires some detailed knowledge of the governing equations. However, at this point it is worth discussing what is known of MHD jets.

Perhaps the earliest analysis of a submerged jet in a static magnetic field is that due to Moreau (1963*a*, *b*). He considered the development of a steady two-dimensional jet (a sheet) under the influence of a uniform transverse magnetic field. The flow was taken as laminar and Moreau was able to obtain an exact solution of the Navier–Stokes equations. This solution revealed that the Lorentz force destroys the jet momentum and that, rather surprisingly, the jet is completely annihilated within a finite distance of its source. Moffatt & Toomre (1967) also investigated this problem, focusing particularly on inviscid jets. Again, it was found that the jet momentum is completely destroyed within a finite distance. Elements of these studies were later extended to two-dimensional turbulent jets by Bansal & Gupta (1978).

These two-dimensional jets are singular in at least one respect. They involve a current which flows only in a plane normal to the jet (parallel to the sheet). Consequently, it is unnecessary, in a mathematical sense, to specify return paths for the induced current. In this paper we consider the development of three-dimensional jets.

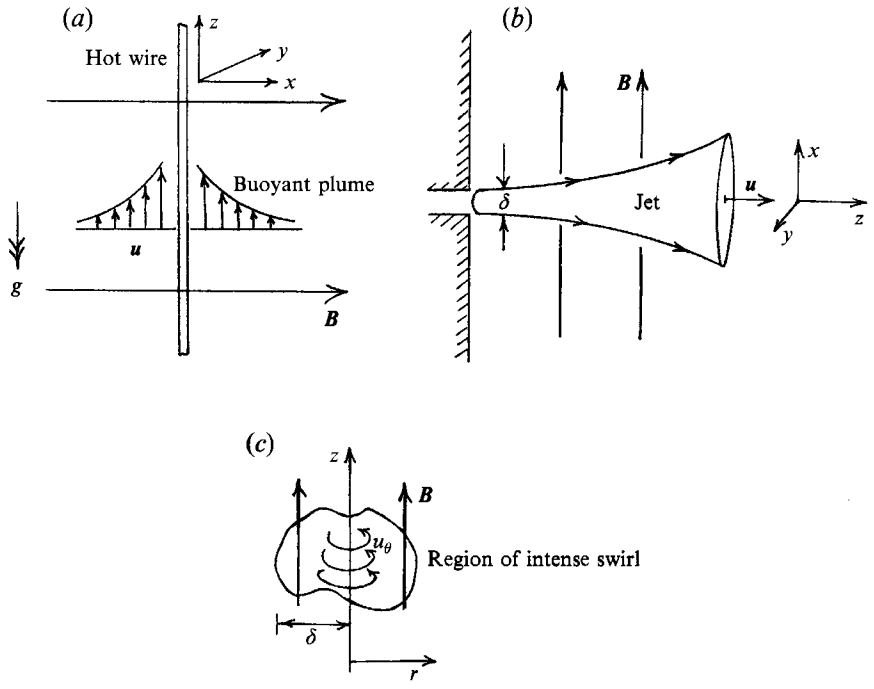

FIGURE 1. Examples of magnetic damping of liquid-metal flows: (*a*) a buoyant plume is generated by a hot wire and a magnetic field is then imposed which dissipates the jet; (*b*) a jet is created by injecting fluid at the boundary; (*c*) a magnetic field dissipates an isolated vortex.

These may start out as axisymmetric, but soon develop a more complex structure. As noted by Moffatt & Toomre (1967), such jets behave quite differently from their two-dimensional counterparts. In particular, it is now necessary to consider how, through the action of a distributed electrostatic potential, the induced current recirculates within the bulk of the liquid. This closing of the current paths has a profound influence on the development of the jet. It is no longer possible to destroy momentum, as occurs in a two-dimensional jet. Rather, the Lorentz force redistributes linear momentum in such a way as to reduce the kinetic energy of the flow. One consequence of conservation of linear momentum is that, in contrast with the two-dimensional case, a three-dimensional jet cannot be destroyed by a magnetic field.

An analogous process occurs in the magnetic damping of vortices. Here, closing of the current lines ensures that at least one component of the angular momentum is conserved. Consequently, the Lorentz force acts to redistribute the angular momentum in such a way as to reduce the kinetic energy of the vortex. However, conservation of angular momentum places a lower bound on the global kinetic energy of the flow, and so, just as with a jet, the vortex cannot be destroyed by magnetic damping.

The structure of the paper is as follows. In §2, we introduce a number of simplifying assumptions. Like Moffatt & Toomre (1967), we take the Reynolds number to be high, so that the flow may be treated as inviscid, and the magnetic Reynolds number be low, so that perturbations to the applied magnetic field may be neglected. Fortuitously, such a parameter regime is typical of many industrial processes. Next, in §3.1, we outline the integral characteristics of three-dimensional magnetic damping. In particular, we show that the Lorentz force does not alter the global momentum of a fluid (angular or linear), although it does destroy kinetic energy. Moreover, the Lorentz force causes the

flow to evolve in such a way as to minimize its global Joule dissipation, and it does this by propagating momentum and vorticity out along the magnetic field lines, a process which is familiar in the context of MHD turbulence. In §3.2 we discuss the distinction between this interpretation of Ohmic damping, which is essentially a global one, based on the conservation or evolution of certain integral characteristics of the flow, and the classic interpretation of MHD turbulence which is local in nature, based on the vorticity transport equation. This distinction is made clear in §3.3, with the aid of the simple example of flow in a sphere.

In the remaining sections we illustrate these rather general observations with a number of specific examples. In increasing order of complexity we look at a spatially uniform jet evolving in time, a steady jet evolving in space, and finally, an axisymmetric vortex evolving in both space and time.

Our first example is somewhat idealized and mathematically rather trivial. Nevertheless, it does capture the essential features of magnetic damping in a simple transparent way, and so provides a useful stepping-stone to related more complex examples. Here a transverse magnetic field is suddenly applied to jet which is initially axisymmetric (figure 1*a*). The jet may be isothermal, or else maintained by buoyancy. We ignore streamwise variations in the jet velocity, so that, at each instant, all cross-sections of the jet look the same. The resulting problem is linear. This simple flow captures the key role played by the current return paths in conserving or maintaining momentum, and in minimizing the global Joule dissipation.

Our second problem is closely related to the first, but is mathematically more complex. In brief, it is the three-dimensional counterpart of the two-dimensional jets (sheets) of Moreau (1963*a*, *b*) and of Moffatt & Toomre (1967). Here an (initially) axisymmetric jet is created by injecting fluid through an aperture in a sidewall (figure 1*b*). Although this is a steady problem, there is a direct analogy between the spatial development of this flow and the temporal evolution of our first example.

Our final, and most complex, example is the damping of axisymmetric vortices (figure 1*c*). Rather surprisingly, there is a qualitative analogy between this flow and the jet flows described above. Angular momentum now plays the role previously occupied by linear momentum. In particular, it is globally conserved and propagates along the magnetic fields lines. The mechanism of propagation is essentially the same as for linear momentum.

2. Simplifying assumptions and governing equations

Suppose that our liquid metal has thermal diffusivity α, electrical conductivity σ, and density ρ. Also, let it occupy a domain V which is infinite, or else is bounded by an electrically insulating surface S. For jet-like flows we shall adopt Cartesian coordinates (x, y, z) with the jet directed along the z-axis, and an imposed, uniform magnetic field, $\boldsymbol{B}$, applied in the x-direction. The jet may be driven by injecting fluid through the boundary, or else take the form of a spatially uniform stream, possibly driven by buoyancy (see figure 1). In cases where the jet is thermally driven, we take z to point vertically upward. Let the velocity field be $\boldsymbol{u}$, the current density be $\boldsymbol{J}$, and the characteristic thickness of the jet or vortex be δ.

It is informative to estimate the time it takes the Lorentz force to decelerate a typical fluid particle. In the absence of an applied electric field, Ohm's law gives $J \sim \sigma u B$, and so the Lorentz force per unit mass becomes

$$\boldsymbol{F} = \boldsymbol{J} \times \boldsymbol{B}/\rho \sim -(\sigma B^2/\rho)\,\boldsymbol{u}.$$

Buoyancy and pressure forces apart, the particle decelerates according to

$$\frac{\mathrm{D}\boldsymbol{u}}{\mathrm{D}t} \sim -(\sigma B^2/\rho)\,\boldsymbol{u}.$$

Clearly, the Lorentz force acts on a time scale of

$$\tau = \rho/(\sigma B^2). \tag{2.1}$$

We now place some restrictions on the magnitude of τ. We shall assume that τ is much greater than δ/u, yet much smaller than the diffusive time scale, δ^2/α. That is,

$$\delta/u \ll \tau \ll \delta^2/\alpha. \tag{2.2a}$$

The first of these inequalities may be rewritten as

$$N = \sigma B^2 \delta/(\rho u) \ll 1. \tag{2.2b}$$

In the conventional nomenclature of MHD, this represents the case of a low magnetic interaction parameter. The second of the inequalities in (2.2) implies that, for buoyant jets, the temperature field may be considered as 'frozen' in the fluid on a time scale of τ. Consequently, if we suddenly apply a $\boldsymbol{B}$-field to a buoyant jet, we may neglect thermal diffusion during the process of magnetic damping.

We shall make two further assumptions. It is convenient to take the Reynolds number to be high, so we may treat the fluid as inviscid, and the magnetic Reynolds number to be low, so that perturbations to the imposed $\boldsymbol{B}$-field may be neglected:

$$Re = u\delta/\nu \gg N^{-1} \gg 1, \tag{2.3a}$$

$$Re_m = \mu\sigma u\delta \ll 1. \tag{2.3b}$$

Expression (2.3a) implies that viscous forces are much smaller than the Lorentz force, while (2.2b) states that inertia is much greater than $\boldsymbol{J}\times\boldsymbol{B}$.

The limitations imposed by (2.2) and (2.3) are not, in fact, overly restrictive. Consider, for example, a 1 cm diameter jet of steel passing through a magnetic field of 0.1 T at a speed of 10 cm s^{-1}. Typical thermophysical properties for steel are: $\sigma = 0.7\times10^6\ \Omega^{-1}\ \mathrm{m}^{-1}$, $\rho = 7\times10^3\ \mathrm{kg\ m}^{-3}$, $\alpha = 5\times10^{-6}\ \mathrm{m}^2\ \mathrm{s}^{-1}$, and $\nu = 10^{-6}\ \mathrm{m}^2\ \mathrm{s}^{-1}$. In this case our various dimensionless groups have values of

$$\delta^2/\alpha\tau = 20; \quad N = 0.1; \quad Re = 10^3; \quad Re_m = 0.9\times10^{-3}.$$

Clearly, inequalities (2.2) and (2.3) are (almost) satisfied.

We may now write down a simplified set of governing equations. By virtue of (2.3b), Ohm's law becomes

$$\boldsymbol{J} = \sigma(-\nabla\Phi + \boldsymbol{u}\times\boldsymbol{B}), \tag{2.4}$$

where Φ is the electrostatic potential, and $\boldsymbol{B}$ is the unperturbed uniform magnetic field. Given $\boldsymbol{u}$, we may determine both $\boldsymbol{J}$ and Φ from (2.4). Since $\boldsymbol{J}$ is solenoidal, Φ is determined by the divergence of (2.4):

$$\nabla^2\Phi = \boldsymbol{B}\cdot\boldsymbol{\omega}, \tag{2.5}$$

where $\boldsymbol{\omega}$ is the vorticity. Taking the curl of (2.4), on the other hand, furnishes an expression for $\boldsymbol{J}$:

$$\nabla\times\boldsymbol{J} = \sigma\boldsymbol{B}\cdot\nabla\boldsymbol{u}. \tag{2.6}$$

Note that the current is linear in $\boldsymbol{u}$ and disappears only when the motion is uniform along the fieldlines. This current gives rise to a Lorentz force per unit mass, $\boldsymbol{F}$, of

$$\boldsymbol{F} = \frac{\boldsymbol{J}\times\boldsymbol{B}}{\rho} = -\frac{\boldsymbol{u}_\perp}{\tau} + \frac{\sigma(\boldsymbol{B}\times\nabla\Phi)}{\rho}, \tag{2.7}$$

where $\boldsymbol{u}_\perp = (0, u_y, u_z)$. Clearly, in the absence of an electrostatic potential, both the y- and z- components of momentum experience a decelerating force of $-\boldsymbol{u}_\perp/\tau$. This is what happens in the two-dimensional jets of Moreau (1963*a*, *b*) and of Moffatt & Toomre (1967). However, we shall see later that the potential Φ is non-zero in three-dimensional flows, and that this has a profound influence on the evolution of the motion. Note that we may eliminate Φ from (2.7) by taking the curl of this expression:

$$\nabla \times \nabla \times \boldsymbol{F} = \frac{B}{\rho}\frac{\partial}{\partial x}(\nabla \times \boldsymbol{J}) = \frac{1}{\tau}\frac{\partial^2 \boldsymbol{u}}{\partial x^2}. \tag{2.8}$$

Let us now turn to the equation of motion for the liquid. In the interests of generality, we shall include a buoyancy term. Neglecting viscous shear stresses, we have

$$\frac{\mathrm{D}\boldsymbol{u}}{\mathrm{D}t} = -\nabla\left(\frac{p}{\rho}\right) + g\beta T\hat{\boldsymbol{e}}_z + \boldsymbol{F}; \quad \nabla\cdot\boldsymbol{u} = 0, \tag{2.9}$$

where T is the temperature, β is the expansion coefficient, and we have used the Boussinesq approximation for the buoyancy force. Using (2.8), we may rewrite this in terms of $\boldsymbol{u}$:

$$\nabla^2\left[\frac{\mathrm{D}\boldsymbol{u}}{\mathrm{D}t}\right] - \nabla\left[\frac{\partial^2(u_i u_j)}{\partial x_i \partial x_j}\right] = -(g\beta)\nabla \times \nabla \times [T\hat{\boldsymbol{e}}_z] - \frac{1}{\tau}\frac{\partial^2 \boldsymbol{u}}{\partial x^2}. \tag{2.10}$$

For isothermal jet flows, where the dominant velocity is u_z, this simplifies to

$$\frac{\mathrm{D}u_z}{\mathrm{D}t} = -\frac{1}{\tau}\nabla_{xy}^{-2}\left[\frac{\partial^2 u_z}{\partial x^2}\right]. \tag{2.11}$$

This suggests that there is a similarity between a spatially uniform jet evolving in time ($\mathrm{D}u_z/\mathrm{D}t = \partial u_z/\partial t$), and a steady jet evolving in space ($\mathrm{D}u_z/\mathrm{D}t = \boldsymbol{u}\cdot\nabla u_z$). We shall see that this is indeed the case.

Finally, we need to choose a datum for T. The only case where we shall allow for buoyancy is the jet-like flow shown in figure 1(*a*). Here it is natural to choose T to be zero in the far field. Now in jet flows the pressure gradient in (2.9) disappears and, as we shall see, the volume integral of the Lorentz force is also zero. Consequently, isothermal jets conserve momentum, while the momentum in a thermally driven jet increases monotonically. (Actually, the choice of datum for T turns out to be rather unimportant. Switching datum merely adds or subtracts a uniform pressure gradient to (2.9). This, in turn, simply implies a uniform acceleration of the flow, depending on how the pressure is chosen at infinity. In the linear problem shown in figure 1(*a*), superposition applies, and so consequently, changing the datum for T merely adds or subtracts a uniform acceleration. This does not alter the way in which the flow develops, other than in a trivial sense.)

We shall now establish some of the more general properties of flows governed by (2.10).

3. An integral approach to magnetic damping

3.1. *Conservation of momentum, destruction of energy, and evolution to minimize dissipation*

Expressions (2.8) and (2.9) exhibit a number of interesting yet rather general features. We shall identify these here, before looking at specific examples of magnetic damping. This will help establish some of the recurring themes which will emerge in subsequent sections.

The essential point is this. A closed current loop, for example a wire, which is situated in a uniform magnetic field experiences a magnetic torque which is perpendicular to $\boldsymbol{B}$. However, it experiences no net force. (See, for example, Jackson 1962.) Since an arbitrary distribution of $\boldsymbol{J}$ may be considered as the superposition of such current loops, the Lorentz force cannot alter the global linear momentum of a fluid, nor can it change the component of angular momentum parallel to $\boldsymbol{B}$. Now this is important because, in certain inviscid flows, the mechanical forces do not change the linear momentum of the fluid (e.g. in isothermal jet flows), while in others the mechanical forces do not change the angular momentum (e.g. flow in a sphere). In such cases, the linear or angular momentum is conserved during magnetic damping, despite the Joule dissipation. This implies that magnetic damping cannot completely destroy the flow. Rather, it redistributes the linear or angular momentum in such a way as to reduce the kinetic energy of the motion.

The nature of this redistribution can be deduced from (2.6). Since $\boldsymbol{J}$ is linear in $\boldsymbol{u}$, we might anticipate that the integral of the Joule dissipation is of the order of E, the kinetic energy of the flow. If this were so, then (buoyancy forces apart) E would decay according to

$$\frac{\mathrm{d}E}{\mathrm{d}t} \sim -E$$

and eventually the flow would be annihilated. As this contravenes conservation of momentum, the fluid must find some means of lowering its Joule dissipation. The key lies in (2.6). The dissipation can be reduced by redistributing the fluid momentum more uniformly along the $\boldsymbol{B}$-lines. Indeed, when the flow is perfectly uniform along the field lines the Joule dissipation is zero. This spreading of angular or linear momentum along the $\boldsymbol{B}$-lines manifests itself repeatedly in the examples which follow.

Let us now quantify these arguments. There are three results which we shall prove. First, although the Lorentz force destroys kinetic energy, the net linear momentum remains unchanged, as does the component of angular momentum parallel to $\boldsymbol{B}$. Second, these flows evolve so as to minimize their Joule dissipation. More precisely, the ratio of the Joule dissipation to the kinetic energy falls as the flow evolves. This is essential to conserving or (for buoyant jets) maintaining the momentum of the flow. Third, the reduction in dissipation is achieved by propagating linear or angular momentum out along the field lines. In the case of a jet, the flow does this by elongating its cross-section in the direction of the $\boldsymbol{B}$-lines. Similarly, a region of intense vorticity spreads along the field lines.

The first of these results is readily established. From (2.4) and (2.7) we have

$$\boldsymbol{F}\cdot\boldsymbol{u} = -\boldsymbol{J}^2/(\rho\sigma) - \nabla\cdot[\Phi\boldsymbol{J}/\rho]$$

from which we obtain the well-known result

$$\int_V \boldsymbol{F}\cdot\boldsymbol{u}\,\mathrm{d}V = -(\rho\sigma)^{-1}\int_V \boldsymbol{J}^2\,\mathrm{d}V. \tag{3.1}$$

That is, the global work performed by the Lorentz force is always negative. We can imbed this in a mechanical energy equation by taking the product of (2.9) with $\boldsymbol{u}$ and integrating over the volume V:

$$\frac{\mathrm{d}E}{\mathrm{d}t} = -\oint_S H\boldsymbol{u}\cdot\mathrm{d}\boldsymbol{S} - (\rho\sigma)^{-1}\int_V \boldsymbol{J}^2\,\mathrm{d}V + g\beta\int_V Tu_z\,\mathrm{d}V. \tag{3.2}$$

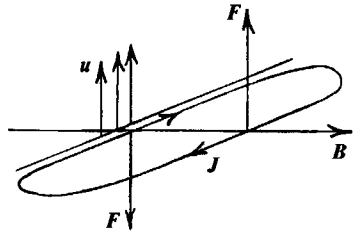

FIGURE 2. The current J consists of closed loops, so if the fluid is locally decelerated at one point, it must be accelerated at another.

Here H is Bernoulli's coefficient and E is the global kinetic energy per unit mass of the fluid. In this paper, we consider cases where the last integral on the right is positive (i.e. thermally driven jets). Consequently, in the absence of a mass flux through the surface S, we may rewrite (3.2) in the form

$$\frac{\mathrm{d}E}{\mathrm{d}t} = g\beta \int_V T u_z \,\mathrm{d}V - (\rho\sigma)^{-1} \int_V J^2 \,\mathrm{d}V = G - D. \tag{3.3}$$

Here G is the generation of energy and D is the global dissipation. In the absence of buoyancy, E decays monotonically. However, this fall in kinetic energy is not matched by a corresponding fall in linear momentum. This becomes evident if we note that,

$$\int_V J_i \,\mathrm{d}V = \int_V \nabla\cdot(x_i \boldsymbol{J}) \,\mathrm{d}V = 0$$

from which we obtain the well-known result

$$\int_V \boldsymbol{F} \,\mathrm{d}V = -\boldsymbol{B} \times \int \boldsymbol{J} \,\mathrm{d}V = \boldsymbol{0}. \tag{3.4}$$

For every fluid element which is decelerated by $\boldsymbol{F}$, there is a corresponding element which receives an equal and opposite acceleration. This is a direct consequence of insisting that the current paths close within V. (See figure 2.) The fact that $\boldsymbol{F}$ cannot create or destroy global momentum is particularly important for jet flows. In isothermal jets it implies that momentum is conserved, while in buoyant jets the momentum increases. In either case, momentum is maintained in the face of Joule dissipation.

It is not difficult to show that a similar result holds for angular momentum. The magnetic torque is

$$\boldsymbol{T} = \boldsymbol{x} \times \boldsymbol{F} = \rho^{-1}[(\boldsymbol{x}\cdot\boldsymbol{B})\boldsymbol{J} - (\boldsymbol{x}\cdot\boldsymbol{J})\boldsymbol{B}].$$

We are interested particularly in the component of $\boldsymbol{T}$ which is parallel to $\boldsymbol{B}$:

$$\boldsymbol{T}\cdot\boldsymbol{B} = -(B^2/\rho)(\boldsymbol{x}_\perp \cdot \boldsymbol{J}_\perp) = -(B^2/2\rho)\nabla\cdot[x_\perp^2 \boldsymbol{J}].$$

Evidently, this integrates to zero, implying that the Lorentz force cannot create or destroy this component of angular momentum. One physical interpretation of this result is to consider each current 'tube' to be the sum of an infinite number of infinitesimal current loops, as in the conventional proof of Stokes theorem. Then each elemental current loop experiences a torque of

$$\mathrm{d}\boldsymbol{T} = (\mathrm{d}\boldsymbol{m}) \times \boldsymbol{B},$$

where $\mathrm{d}\boldsymbol{m}$ is its dipole moment. The net torque on each current tube is then

$$\boldsymbol{T} = \sum \mathrm{d}\boldsymbol{m} \times \boldsymbol{B},$$

which clearly has no component parallel to $\boldsymbol{B}$. This result is crucially important for vortical flows, yet it seems to have been largely overlooked in the literature on magnetic damping.

Consider now our second assertion: that the flow evolves so as to minimize its Joule dissipation. Our starting point is the rate of change of dissipation. Noting that

$$(\rho\sigma)^{-1}\boldsymbol{J}\cdot\frac{\partial \boldsymbol{J}}{\partial t} = -\boldsymbol{\nabla}\cdot\left[\frac{\boldsymbol{J}\partial\boldsymbol{\Phi}}{\rho\,\partial t}\right] - \boldsymbol{F}\cdot\frac{\partial \boldsymbol{u}}{\partial t}$$

we may express the rate of change of D in the form

$$\frac{\mathrm{d}D}{\mathrm{d}t} = -2\int_V \boldsymbol{F}\cdot\frac{\partial \boldsymbol{u}}{\partial t}\,\mathrm{d}V. \tag{3.5}$$

We are also interested in the rate of change of relative dissipation, D/E. From (3.3) and (3.5) we have

$$E^2\frac{\mathrm{d}}{\mathrm{d}t}\left(\frac{D}{E}\right) = \left[\int_V \boldsymbol{F}\cdot\boldsymbol{u}\,\mathrm{d}V\right]^2 - \int_V \boldsymbol{u}^2\,\mathrm{d}V\int_V \boldsymbol{F}\cdot\frac{\partial \boldsymbol{u}}{\partial t}\,\mathrm{d}V - DG,$$

which, with the aid of the Schwarz inequality, becomes

$$E^2\frac{\mathrm{d}}{\mathrm{d}t}\left(\frac{D}{E}\right) \leqslant 2E\int_V \boldsymbol{F}\cdot\left(\boldsymbol{F}-\frac{\partial \boldsymbol{u}}{\partial t}\right)\mathrm{d}V - DG. \tag{3.6}$$

Now each flow evolves partially as a result of its own inertia, which depends on its previous history, partially as a result of the buoyancy force, and partially as a result of the Lorentz force. Suppose that, in a time δt, the velocity changes by an amount $\delta\boldsymbol{u}$. Consider only that contribution to $\delta\boldsymbol{u}$ which arises from the Lorentz force,

$$\delta\boldsymbol{u}_F = \boldsymbol{F}\delta t.$$

Then, from (3.5), the corresponding contribution to δD is negative. Clearly, the Lorentz force acts to continually lower the global dissipation. However, this is hardly surprising. Both D and E are quadratic in $\boldsymbol{u}$, so when E declines as a result of Joule dissipation, we would expect D to fall also. The more important and surprising result lies in (3.6). Again, consider only that part of $\delta\boldsymbol{u}$ which is produced by the Lorentz force. The corresponding contribution to the change in relative dissipation, $\delta(D/E)$, is negative. Consequently, to the extent that the Lorentz force influences the flow, the global dissipation declines, and it declines faster than the kinetic energy. We conclude, therefore, that the Lorentz force tends to guide the flow in such a way as to produce a continual reduction in the relative dissipation, D/E. Whether or not the flow is free to follow this 'path of least resistance' depends, of course, on the other forces acting in the fluid. However, in cases where linear or angular momentum is conserved, we may show that the Lorentz force must ultimately win. For example, consider an isothermal flow. Then (3.3) may be integrated to give,

$$E = E_0\exp\left[-\int_0^t (D/E)\,\mathrm{d}t\right],$$

where E_0 is the initial kinetic energy. Now, as we shall see, conservation of momentum

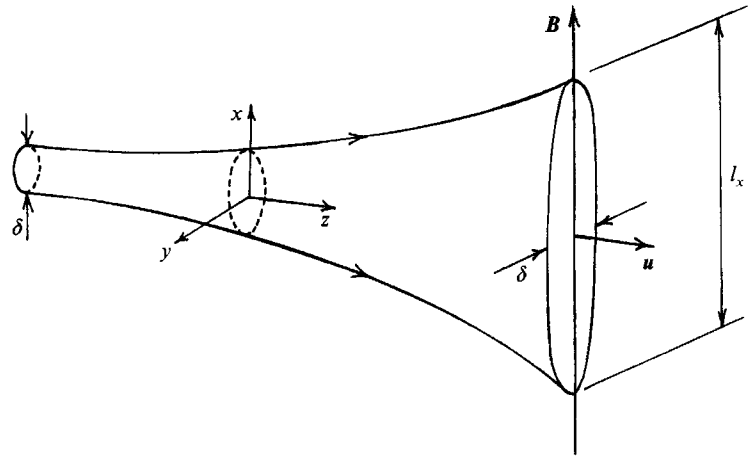

FIGURE 3. A jet can minimize the Joule dissipation by stretching its cross-section along the $\boldsymbol{B}$-lines.

limits the rate of decline of E. In some cases, such as a confined vortex, it implies E is bounded from below (see §3.3). In others, such as an isothermal jet, it implies that E decays algebraically, and not exponentially (see §4). In either situation, this is possible only if the relative dissipation, D/E, decays at large t.

For a buoyant jet the argument must be modified slightly, but the conclusion is broadly similar. In this case we have

$$\dot{E} = -(D/E)E + G,$$

where G is, at most, of order $E^{1/2}$. Now suppose D/E were to remain constant, or else increase with time. Then, as the jet momentum and energy increased under the influence of buoyancy, the first term on the right of our energy equation would increase faster than the second. Eventually, the two terms must become equal and at this point E ceases to grow. However, the jet momentum must continue to rise, implying that the ratio of energy to momentum falls. This is possible only if the jet velocity falls, which is incompatible with an increasing momentum. (This is discussed in more detail in §4.) Once again, we conclude that the relative dissipation declines at large t.

We shall see that this evolution to minimize relative dissipation is a consistent theme of subsequent sections, and that this evolution is inevitably bound up with a 'spreading' of the flow along the $\boldsymbol{B}$-lines. This brings us to our third general result.

A hint as to why elongation of the flow must occur comes from estimating the magnitude of D. From (2.6) we have

$$D \sim (E/\tau)(\delta/l_x)^2, \tag{3.7}$$

where δ is the minimum length scale of the flow and l_x is the characteristic length scale in the direction of $\boldsymbol{B}$. Evidently, if the relative dissipation is to decline, say to preserve momentum, then l_x/δ must increase. Thus a jet whose cross-section is initially axisymmetric can reduce its dissipation, and so help preserve its momentum, by adopting an elongated shape as shown in figure 3. In general, flows which conserve linear or angular momentum must undergo such a distortion in order to survive.

It is informative to estimate the other integrals in the energy equation (3.3). The buoyancy term is of order

$$G \leqslant g\beta T_{rms}(2E)^{1/2} \sim g\beta T_{rms} E^{1/2}, \tag{3.8}$$

where T_{rms} is defined as

$$T_{rms}^2 = \int T^2 \, \mathrm{d}V.$$

Note that T_{rms} has the dimensions of $TL^{3/2}$, and is a constant of the motion when thermal diffusion is neglected. Our energy equation now becomes

$$\mathrm{d}E/\mathrm{d}t \sim g\beta T_{rms} E^{1/2} - (E/\tau)(\delta/l_x)^2. \tag{3.9}$$

The extent to which stretching of a flow can influence its survival can be estimated from (3.9). Consider the case of an axisymmetric jet which is suddenly subject to a transverse magnetic field. If the jet cross-section were to remain axisymmetric, then $\delta \sim l_x$ and (3.9) gives

$$E^{1/2} \sim E_0^{1/2} \, \mathrm{e}^{-t/2\tau} + g\beta T_{rms} \tau [1 - \mathrm{e}^{-t/2\tau}], \tag{3.10}$$

where E_0 is the initial kinetic energy. In cases where the buoyancy force is zero, the jet is dissipated on a time scale of τ. However, this contravenes conservation of momentum, and so clearly $\delta \sim l_x$ is an unphysical option. For a buoyant jet, on the other hand, equation (3.10) implies $E^{1/2}$ saturates at $g\beta T_{rms}\tau$. Once again this constitutes unphysical behaviour, essentially for the reasons discussed above.

Now compare this with the more realistic case where stretching does occur, as indicated schematically in figure 3. For example, suppose the jet cross-section distorts from a circle to a sheet according to

$$l_x^2 = \delta^2(t+\tau)/\tau.$$

Then at large times, (3.9) has solution

$$E^{1/2} \sim E_0^{1/2}(t/\tau)^{-1/2} + \tfrac{1}{3} g\beta T_{rms} \, t. \tag{3.11}$$

The initial jet energy now decays algebraically, as $t^{-1/2}$, rather than exponentially. Such a decay conserves momentum, since $E^{1/2} l_x$ is independent of t. In addition, buoyant jets no longer saturate, but rather grow as $u \sim t$. Evidently, distortion of the jet cross-section substantially enhances the ability of the jet to survive in a magnetic field.

3.2. *Global versus local descriptions of magnetic damping*

In this, and in the subsequent sub-section, we shall show that the interpretation of magnetic damping given above is consistent with, or equivalent to, the classic view of Ohmic damping at large interaction parameter. Moreover, we shall show that our integral interpretation of damping allows us to extend some of the traditional ideas down to small values of the interaction parameter, where the governing equations are usually nonlinear (inertia $\gg$ Lorentz force).

There have been many notable studies of magnetic damping, particularly in the context of MHD turbulence. Typical of these are the work of Moffatt (1967), Alemany *et al.* (1979) and Sommeria & Moreau (1982). It is worth reviewing briefly some of their findings if only to place the subsequent discussion in context. Moffatt analysed the transient decay of turbulence in a strong uniform magnetic field. The interaction parameter was taken as large (the opposite of our case) and as a consequence the momentum equation could be linearized by ignoring advection of momentum. For circumstances in which $Re_m N$ is small, he found that, provided t is greater than τ but much less than the eddy turnover time, the energy decays as $(t/\tau)^{1/2}$. More importantly, a form of two-dimensional flow develops, in the sense that the flow is independent of

the coordinate parallel to $\boldsymbol{B}$. (Curiously, however, the fluctuating component of velocity parallel to $\boldsymbol{B}$ does not tend to zero, but rather increases.) This tendency to promote quasi-two-dimensional turbulence is in accordance with numerous experiments.

Alemany *et al.* (1979) investigated experimentally the case where the interaction parameter took both low and high values. For their particular configuration, which consisted of a grid moving through a magnetic field, they observed a $t^{-1.7}$ decay of energy. This is significantly faster than the decay in the absence of a magnetic field, reflecting the added effect of Joule dissipation. More importantly, they observed an increase in the integral length scale of the turbulence parallel to $\boldsymbol{B}$, indicating an elongation of the turbulent structures in the direction of the $\boldsymbol{B}$-lines. Close to the grid, this increase was rather limited, varying from $\sim 10\%$ to $\sim 80\%$ as the interaction parameter based on the eddy turnover time varied from ~ 0.1 to ~ 1.3. However, as noted by Alemany *et al.*, the local interaction parameter increases as the turbulence decays, essentially because the eddy turnover time increases. Consequently, even in cases where the initial interaction parameter is moderate or small (but not too small), significant elongation of the eddies must eventually occur.

The experiments of Alemany *et al.* are important as they constitute one of the few sets of measurements which are free from the influence of the boundaries. There have been many equivalent experiments performed in ducts (see, for example, Lielausis 1975), and in these cases the boundaries normal to the field can be important. Sommeria & Moreau (1982) and Moreau (1990) discuss the distinction between the two sets of experiments, noting in particular that MHD duct flows are more prone to display two-dimensional characteristics.

The tendency for turbulent structures to lengthen in the direction of the $\boldsymbol{B}$-lines is generally explained in terms of the local vorticity transport equation. (See, for example, Sommeria & Moreau 1982.) Taking the curl of (2.10) gives,

$$\frac{\mathrm{D}\boldsymbol{\omega}}{\mathrm{D}t} = \boldsymbol{\omega}\cdot\boldsymbol{\nabla}\boldsymbol{u} - \frac{1}{\tau}\nabla^{-2}[\partial^2\boldsymbol{\omega}/\partial x^2]. \tag{3.12}$$

Alternatively, we could write the momentum equation in the form (see Sommeria & Moreau)

$$\frac{\mathrm{D}\boldsymbol{u}}{\mathrm{D}t} = -\boldsymbol{\nabla}(P^*/\rho) - \frac{1}{\tau}\nabla^{-2}[\partial^2\boldsymbol{u}/\partial x^2], \tag{3.13}$$

where P^* is the sum of the magnetic pressure and the fluid pressure. If the flow is such that gradients parallel to $\boldsymbol{B}$ are significantly smaller than those in the transverse plane, then (3.12) becomes

$$\frac{\mathrm{D}\boldsymbol{\omega}}{\mathrm{D}t} \sim \boldsymbol{\omega}\cdot\boldsymbol{\nabla}\boldsymbol{u} + \frac{\delta^2}{\tau}\frac{\partial^2\boldsymbol{\omega}}{\partial x^2}, \tag{3.14}$$

where δ is a typical transverse length scale. The implication is that vorticity (and momentum) tends to diffuse parallel to the magnetic field. From a local point of view, therefore, l_x increases owing to pseudo-diffusion, and consequently the relative dissipation, D/E, declines in accordance with (3.7). We might contrast this with our global interpretation, where conservation of momentum places restrictions on the rate of decay of E, which in turn requires D/E to decay, implying an increase in l_x.

It would seem, therefore, that both interpretations come broadly to the same conclusions, albeit from different directions. However, the problem arises when N is

small, so that inertia is much greater than the Lorentz force. The diffusion argument then becomes rather weak. In particular, if there is no significant distinction between transverse and parallel length scales, as would tend to be the case in an inertially dominated turbulent flow, then one cannot strictly infer a diffusion equation like (3.14). In this situation it is usual to take a three-dimensional Fourier transform of (3.12), which indicates that the magnetic field suppresses preferentially those Fourier components of $\boldsymbol{u}$ which have a wave vector parallel to $\boldsymbol{B}$. Now this, in turn, might suggest the development of a two-dimensional flow, as indeed happens when N is large (Moffatt 1967). However, when N is small, the vortex lines stretch and twist on a time scale of δ/u, which is much more rapid than τ. Consequently, while $\boldsymbol{B}$ slowly destroys certain wave-vector components, there is a vigorous redistribution of vorticity and energy between the components, as well as the generation of new vorticity. Recent numerical experiments by Oughton, Priest & Matthaeus (1994) indicate that, for turbulence decaying in a cube, anisotropy develops only when the ratio of the Lorentz force to the inertial forces is near to, or greater than, unity. For low values of this ratio, say 0.1, no isotropy was observed. (However, this may reflect the modest Reynolds number of their computations (typically 200).) In any event, we might conclude that magnetic damping at small N is a non-trivial phenomenon which is still incompletely understood. Certainly, the nonlinear equations (3.12) and (3.13) look quite formidable.

An integral approach, on the other hand, can often furnish some useful information for surprisingly little effort. We shall take the example of flow in a sphere as a vehicle to illustrate the utility of this approach.

3.3. *Flow in a sphere: an illustration of the utility of an integral approach to Ohmic damping*

Suppose the fluid is isothermal and held in a sphere of radius R. At $t = 0$ we specify some quite arbitrary velocity distribution. For example, it may be a complex turbulent flow. Then we can show that, whatever the value of N, the flow evolves to a steady state in which all components of angular momentum are zero, except that which is parallel to $\boldsymbol{B}$. The argument is elementary. We start by noting that neither the Lorentz force nor the pressure forces acting on S contribute to the net torque parallel to $\boldsymbol{B}$. It follows that the global angular momentum of the fluid, $\boldsymbol{H}$, is conserved in the direction of $\boldsymbol{B}$. This, in turn, places a lower bound on the kinetic energy of the flow. In particular, the Schwarz inequality gives us

$$E \geqslant H_B^2 \Big/ \left[2 \int x_\perp^2 \, \mathrm{d}V\right], \tag{3.15}$$

where H_B is the component of angular momentum parallel to $\boldsymbol{B}$. Provided H_B is non-zero, the flow cannot come to rest. Yet (2.6) tells us that as long as there is some variation in velocity along the $\boldsymbol{B}$-lines, the Joule dissipation remains finite and E continues to fall. Consequently, whatever the initial condition, the flow must evolve to a steady state which is strictly two-dimensional, exhibiting no variation of $\boldsymbol{u}$ along the field lines. Moreover, this steady state must have the same angular momentum, H_B, as the initial flow. In short, the flow adopts the form of one or more columnar vortices, each aligned with the $\boldsymbol{B}$-field, all other components of angular momentum having been destroyed. Of course, during this process the relative dissipation decays to zero, while the characteristic length scale l_x increases in accordance with (3.7). All-in-all, the picture is much as described in §3.1.

Now the arguments above hold not just for a sphere, but for any axisymmetric container which has the symmetry axis aligned with $\boldsymbol{B}$. Also, they hold for any value

of N, and in particular for small N where inertia is dominant. It is rather striking that such a simple steady state emerges even when stretching and twisting of vorticity is more vigorous than damping or pseudo-diffusion induced by $\boldsymbol{B}$. It is not obvious that we could reach the same conclusions by inspection of the vorticity equation, particularly as this equation places no lower bound on E. (It is possible to construct a naive argument based on the local equations, as follows. As the motion decays, the eddy turnover time rises, so that the effective interaction parameter increases. When N exceeds a value of around unity the equations become almost linear and diffusion-like elongation of the eddies sets in. However, since E is bounded from below, this argument fails. Clearly, a more sophisticated line of reasoning is required.)

Now the integral equations also furnish information on the transient behaviour of this flow. The most direct route is to determine the evolution of the angular momentum vector, and then use this to infer the changes in energy and vorticity. Our starting point is the magnetic torque, which may be written as

$$\boldsymbol{T} = \frac{1}{\rho}\int_V \boldsymbol{x}\times(\boldsymbol{J}\times\boldsymbol{B})\,\mathrm{d}V = \frac{1}{2\rho}\int_V [(\boldsymbol{x}\cdot\nabla\times\boldsymbol{J})\boldsymbol{x}]\,\mathrm{d}V\times\boldsymbol{B}$$

Here we have used the identity

$$2\boldsymbol{x}\times\boldsymbol{F}_i = (\boldsymbol{x}\cdot\nabla\times\boldsymbol{J})(\boldsymbol{x}\times\boldsymbol{B})_i + \nabla\cdot[(\boldsymbol{x}\times(\boldsymbol{x}\times\boldsymbol{B}))_i\boldsymbol{J} + (\boldsymbol{x}\times\boldsymbol{B})_i\,\boldsymbol{x}\times\boldsymbol{J}].$$

We now substitute for $\boldsymbol{J}$ using (2.6). This furnishes an expression for the net torque in terms of the global angular momentum:

$$\boldsymbol{T} = \frac{\sigma B}{2\rho}\int_V \left(\boldsymbol{x}\cdot\frac{\partial\boldsymbol{u}}{\partial x}\right)\boldsymbol{x}\,\mathrm{d}V\times\boldsymbol{B} = -\frac{\boldsymbol{H}_\perp}{4\tau}. \tag{3.16}$$

Again we have used a vector identity, in the form

$$\left(\boldsymbol{x}\cdot\frac{\partial\boldsymbol{u}}{\partial x}\right)(\boldsymbol{x}\times\boldsymbol{B})_i = \nabla\cdot[(\boldsymbol{x}\cdot\boldsymbol{u})(\boldsymbol{x}\times\boldsymbol{B})_i\,\hat{\boldsymbol{e}}_x - \tfrac{1}{2}x(\boldsymbol{x}\times\boldsymbol{B})_i\,\boldsymbol{u}] - \tfrac{1}{2}B(\boldsymbol{x}\times\boldsymbol{u})_\perp.$$

It follows that the global angular momentum equation is,

$$\frac{\mathrm{d}\boldsymbol{H}}{\mathrm{d}t} = -\frac{\boldsymbol{H}_\perp}{4\tau} \tag{3.17}$$

so that transverse components of $\boldsymbol{H}$ decay as

$$\boldsymbol{H}_\perp = \boldsymbol{H}_{\perp 0}\exp[-t/4\tau]. \tag{3.18}$$

It is tempting to conclude that the steady state must also be reached on a time scale of 4τ. However, this need not be so, and indeed we shall give a counter example in §6. We can show, however, that the initial decay in 'excess' energy (initial minus final energy) is at least as fast as the decline in the transerse components of $\boldsymbol{H}$. The approach is to place a lower bound on the dissipation integral and then use the energy equation (3.3) to bound E from above. This procedure will also provide an upper bound for the rate of growth of the longitudinal lengthscale l_x. We start by introducing vector potentials for $\boldsymbol{J}$ and $\boldsymbol{u}$, defined via the Biot–Savart law. For example, for $\boldsymbol{J}$ we have

$$\nabla\times\boldsymbol{b} = \boldsymbol{J}, \quad \boldsymbol{b} = \frac{1}{4\pi}\int(\boldsymbol{J}'\times\boldsymbol{s})\,s^{-3}\,\mathrm{d}V',$$

where $s = x - x'$. We define the vector potential for the velocity field, a, in precisely the same way, and this us allows to write

$$\lambda_0^2 \int_V b^2 \, dV \leqslant \int_V J^2 V \leqslant \sigma^2 B^2 \int_V (\partial a/\partial x)^2 \, dV. \tag{3.19}$$

The first of these inequalities may be established using the calculus of variations (see, for example, Roberts 1967). It turns out that λ_0^2 is the least eigenvalue of a simple eigenvalue problem, the details of which need not concern us here. The second inequality comes from 'uncurling' (2.6) to give

$$\sigma B \frac{\partial a}{\partial x} = J + \nabla\phi, \quad \nabla^2\phi = 0.$$

Next we note that, since J is restricted to a sphere, we have the standard result

$$\int b \, dV \times B = \frac{1}{3}\int (x \times J) \, dV \times B = \tfrac{2}{3}\rho T.$$

(See, for example, Jackson 1962.) This, with the aid of (3.16), furnishes a simple expression for the integral of the vector potential b in terms of H:

$$\int_V b_\perp \, dV = \tfrac{1}{6}\sigma H \times B.$$

This equation now provides a lower bound for the left-hand integral in (3.19), and thus provides the required lower bound on global dissipation:

$$\frac{\lambda_0^2 H_\perp^2}{36\tau V} \leqslant D \leqslant \frac{2E}{\lambda_0^2 \tau l_x^2}. \tag{3.20}$$

Here we have found it convenient to define the longitudinal length scale l_x in terms of a, according to

$$l_x^2 \int_V (\partial a/\partial x)^2 \, dV = \int_V a^2 \, dV \leqslant \lambda_0^{-2} \int_V u^2 \, dV.$$

Expression (3.20) places an upper bound on l_x, and hence an upper bound on the rate of elongation of the flow. More significantly, it provides the key result needed to estimate the decay in excess energy. Substituting the lower bound for D in energy equation (3.3) gives

$$\Delta E = E_0 - E \geqslant \frac{2\lambda_0^2 H_{\perp 0}^2}{9V}[1 - \exp(-t/8\tau)]. \tag{3.21}$$

We conclude, therefore, that the decay in E is at least as rapid as the decay in the transverse components of angular momentum.

Finally, it is natural to associate angular momentum with vorticity. We might anticipate, therefore, that a knowledge of the decline in H should shed light on the suppression of the transverse components of vorticity. In an integral sense this is indeed the case, as we have

$$H = \frac{1}{2}\int (R^2 - x^2)\omega \, dV. \tag{3.22}$$

However, just as with (3.18), this does not guarantee that ω everywhere approaches a

steady state on the time scale of 4τ. In fact, in general it does not. To obtain information about the decline in the *local* vorticity distribution we need to look at the enstrophy. The Schwarz inequality applied to (3.22) gives

$$\int \omega_i^2 \, \mathrm{d}V \geqslant 7H_i^2/R^2 I. \tag{3.23}$$

Here I is the moment of inertia of the liquid, and (3.23) may be applied to each component of enstrophy in turn. Of particular interest is the component of enstrophy parallel to $\boldsymbol{B}$:

$$\int \omega_B^2 \, \mathrm{d}V \geqslant 7H_B^2/R^2 I.$$

This, like (3.15), confirms that the steady state is non-trivial. Evidently, an integral analysis furnishes a great deal of useful information, and for relatively little effort. Given that the interaction parameter may be small, so that the governing equations are nonlinear, this is somewhat surprising.

3.4. *Damping of more complex flows*

Of course, motion in a sphere is rather a particular case, and is hardly characteristic of the types of engineering flows discussed in § 1. In more complex flows, the integral equations alone are not sufficient to describe Ohmic damping. In the examples which follow, which are more characteristic of engineering applications, we shall find it both useful and necessary to employ local (diffusion-like) arguments as well as integral constraints. Nevertheless, we shall see that our global interpretation of damping does provide a useful framework for interpreting a range of problems. All of the examples which follow are characterized by: (*a*) the need to maintain momentum in the face of Joule dissipation; (*b*) a decay in relative dissipation just sufficient to maintain momentum; and (*c*) a gradual elongation of the flow along the $\boldsymbol{B}$-lines which allows D/E to fall.

The three flows which we shall examine are all shown in figure 1. We start with a spatially uniform jet which is dissipated by the sudden application of a transverse magnetic field (figure 1 *a*). This is mathematically rather trivial but provides a useful stepping-stone to our second example of a steady jet evolving in space (figure 1 *b*). This second flow is relevant to mould filling in the casting industry. For our final example we return to the topic of magnetic damping of vortices. Here we focus on axisymmetric flows as this allows us to examine the interaction of damped and undamped components of motion.

4. Example 1. Transient magnetic damping of a spatially uniform jet

Suppose we have a unidirectional flow, $\boldsymbol{u} = u(x, y, t)\,\hat{\boldsymbol{e}}_z$, which is initially axisymmetric and localized near the origin. This is illustrated in figure 4(*a*). The jet may be isothermal, or else driven by buoyancy. Since the flow starts as axisymmetric, it is convenient to introduce polar coordinates, r and θ, in the (x, y)-plane. Physically, such a flow could be generated as shown in figure 1(*a*), where heat is allowed to diffuse out of a long hot wire for an extended period of time (greater than τ).

At $t = 0$ we impose a uniform magnetic field, $\boldsymbol{B} = B\hat{\boldsymbol{e}}_x$. This, in turn, induces a current which is confined to the (x, y)-plane, as shown in figure 4(*b*). The current is driven in the y-direction by $\boldsymbol{u} \times \boldsymbol{B}$, but is forced to recirculate back through regions of

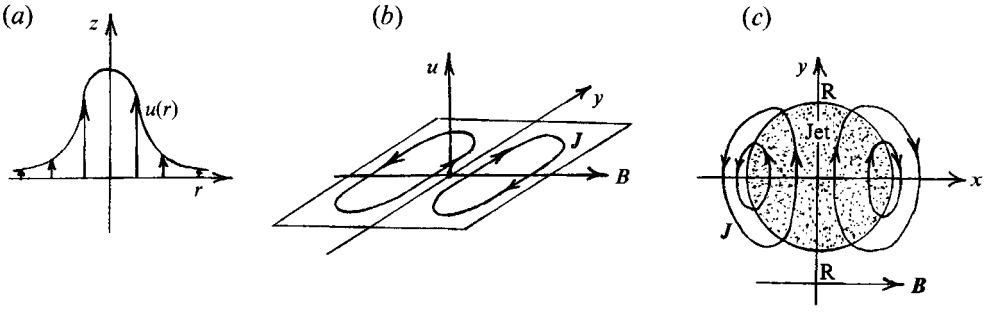

FIGURE 4. Magnetic damping of a uniform jet: (*a*) initial axisymmetric velocity profile; (*b*) the induced current; and (*c*) current flow in the (x, y)-plane. A reverse flow forms at points marked R.

weak or zero flow by the electrostatic potential (figure 4*c*). Since the current is two-dimensional, we can introduce a streamfunction for J, defined through

$$J = \sigma B \nabla \times [\psi \hat{e}_z]. \tag{4.1}$$

Ohm's law, in the form of (2.6), then requires

$$\nabla^2 \psi = -\partial u/\partial x. \tag{4.2}$$

The Lorentz force is simply

$$F = \frac{1}{\tau}\frac{\partial \psi}{\partial x}\hat{e}_z \tag{4.3}$$

and so the equation of motion reduces to

$$\frac{\partial u}{\partial t} = \frac{1}{\tau}\frac{\partial \psi}{\partial x} + g\beta T. \tag{4.4}$$

We can eliminate ψ from this expression with the aid of (4.2), to produce a one-dimensional version of (2.10):

$$\nabla^2\left(\frac{\partial u}{\partial t}\right) = -\frac{1}{\tau}\frac{\partial^2 u}{\partial x^2} + g\beta\nabla^2 T. \tag{4.5}$$

This equation is linear and so is readily solved for u. However, inspection of (4.4), in conjunction with the corresponding energy equation,

$$\frac{\partial}{\partial t}\left(\frac{u^2}{2}\right) = g\beta T u - (\rho\sigma)^{-1} J^2 - \nabla\cdot(\Phi J/\rho), \tag{4.6}$$

furnishes a great deal of useful information without the need to solve (4.5). In particular, we may establish four important features of the flow. First, it is evident that linear momentum is conserved in an isothermal jet. This is a special case of (3.4):

$$\frac{\mathrm{d}}{\mathrm{d}t}\int u \,\mathrm{d}A = \frac{1}{\tau}\int \frac{\partial \psi}{\partial x}\,\mathrm{d}A = 0. \tag{4.7}$$

Second, figure 4(*c*) shows that the returning current at large $|x|$ actually accelerates previously stagnant fluid. This helps conserve global momentum, and is the first hint that energy 'diffuses' out along the x-axis. Third, we would expect regions of reverse flow to form at the points marked R in figure 4(*c*), where the Lorentz force is negative

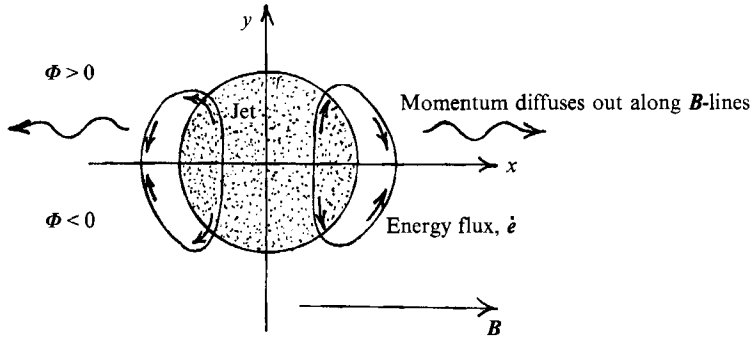

FIGURE 5. Energy flows out along the current lines carrying momentum into previously stagnant regions. In this way momentum diffuses out along the x-axis.

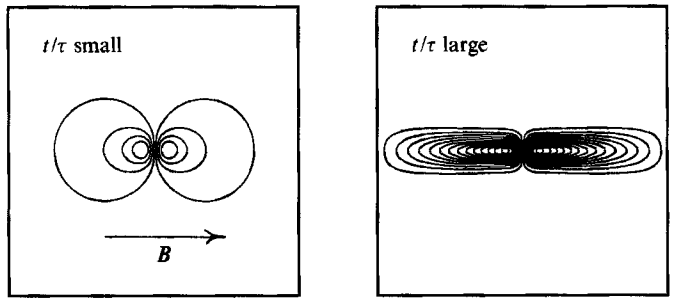

FIGURE 6. Transient magnetic damping of a uniform jet: current distribution at small and large dimensionless times, t/τ.

and the initial jet momentum is small. Finally, the third term in equation (4.6) represents a flux, or redistribution, of energy. Evidently, the kinetic energy flux per unit area is $\Phi \boldsymbol{J}/\rho$, so that energy flows out along the $\boldsymbol{J}$-lines as shown in figure 5. Notice that this flux of energy is directed out of the jet and towards large $|x|$. This is another manifestation of the fact that momentum diffuses out along the field lines.

This propagation of momentum along the $\boldsymbol{B}$-lines is essential to the maintenance of momentum. To see why this is so consider the case of an isothermal jet. We may rewrite (4.5) in the form

$$\nabla^2\left[\frac{\partial u}{\partial t}+\frac{u}{2\tau}\right]=\frac{1}{2\tau}\left(\frac{\partial^2 u}{\partial y^2}-\frac{\partial^2 u}{\partial x^2}\right). \tag{4.8}$$

If the jet were to remain axisymmetric, the right-hand side of this equation would be zero, causing the jet momentum to decay as

$$u\delta^2 \sim u_0\, \mathrm{e}^{-t/2\tau}\delta^2 \tag{4.9}$$

which contravenes conservation of linear momentum.

It is illuminating to consider the influence of this diffusion of momentum on the evolution of the current lines. The development of the current distribution is shown schematically in figure 6. The current starts with a dipole-like shape, characteristic of an isolated jet, and then develops an elongated structure as the jet spreads along the x-axis. This elongation of the J-lines provides the essential mechanism by which the flow minimizes its Joule dissipation. By developing a sheet-like structure, the jet forces

longer and longer return paths on the current. However, the potential difference which drives the current, $uB\delta$, remains the same. The net result is a fall in $|\boldsymbol{J}|$ and a corresponding drop in dissipation. This is consistent with (3.7), in the form

$$D = \tau^{-1} \int_A (\nabla\psi)^2 \, \mathrm{d}A \sim \frac{E}{\tau}(\delta/l_x)^2 \tag{4.10}$$

and ensures that D/E continually falls, as required by (3.6).

We can also determine the asymptotic structure of these jets simply from inspection of the governing equations. The key to understanding this structure is to note that momentum diffuses out along the magnetic field lines, resulting in a continual distortion of the jet cross-section. That this is indeed a diffusive process may be established as follows. For large t, the jet cross-section becomes long and narrow, $l_x \gg \delta$, and so (4.5) simplifies to

$$\frac{\partial}{\partial t}\left(\frac{\partial^2 u}{\partial y^2}\right) = -\frac{1}{\tau}\frac{\partial^2 u}{\partial x^2} + g\beta\nabla^2 T. \tag{4.11}$$

Suppose we now Fourier-transform in the y-direction. Let U be the transformed velocity, and k be the wavenumber. Since the origin of the motion is unimportant to our argument, we shall neglect the buoyancy term. The transformed equation is

$$\frac{\partial U}{\partial t} = \frac{1}{\tau k^2}\frac{\partial^2 U}{\partial x^2} = \alpha_B \frac{\partial^2 U}{\partial x^2}.$$

Thus, as suggested in §3.2, U does indeed diffuse along the $\boldsymbol{B}$-lines, with an effective diffusivity of $\alpha_b \sim \delta^2/\tau$. That momentum can diffuse along a magnetic field line is, of course, well known in the context of MHD turbulence. The process may be regarded as a degenerate form of Alfvén wave propagation, where Re_m is small.

At this point it is convenient to introduce the dimensionless time $\hat{t} = t/\tau$. For large $\hat{t}$, (4.11) suggests that l_x scales as

$$l_x \sim \delta(t/\tau)^{1/2}, \quad \hat{t} \gg 1.$$

We would expect, therefore, that u takes the form

$$u = u(x/\hat{t}^{1/2}, y, \hat{t}), \quad \hat{t} \gg 1. \tag{4.12}$$

In fact, it is not difficult to show that, for infinite domains, that is indeed the case. The most convenient method of establishing u at large times is to use Fourier transforms. Let U be the cosine transform of u,

$$U(k_x, k_y) = 4\int_0^\infty \int_0^\infty u(x,y)\cos(xk_x)\cos(yk_y)\,\mathrm{d}x\,\mathrm{d}y,$$

and let $\Gamma(k)$ be the equivalent transform of $T(r)$. (Here, $k^2 = k_x^2 + k_y^2$.) Our equation of motion, (4.5), now becomes

$$\frac{\partial U}{\partial t} + \cos^2\phi\frac{U}{\tau} = g\beta\Gamma; \quad \cos\phi = k_x/k,$$

from which

$$U(k_x, k_y) = U_0(k)\,\mathrm{e}^{-(\cos^2\phi)\hat{t}} + g\beta\tau\Gamma(k)\frac{1-\mathrm{e}^{-(\cos^2\phi)\hat{t}}}{\cos^2\phi}. \tag{4.13}$$

Here U_0 is the transform of the initial velocity distribution $u_0(x)$. The inverse transform of (4.13) is

$$u(x,t) = \pi^{-2}\int_0^\infty\int_0^{\pi/2} e^{-(\cos^2\phi)\hat{t}}\cos(xk_x)\cos(yk_y)\,U_0(k)\,k\,dk\,d\phi$$

$$+\frac{g\beta\tau}{\pi^2}\int_0^\infty\int_0^{\pi/2}[1-e^{-(\cos^2\phi)\hat{t}}][\cos\phi]^{-2}\cos(xk_x)\cos(yk_y)\,\Gamma(k)\,k\,dk\,d\phi. \quad (4.14)$$

Although this is rather a complex expression, we shall see that it simplifies considerably when t becomes large. In any event, we have a simple relationship for the velocity on the axis:

$$u(0,t) = u_0(0)(2/\pi)\int_0^{\pi/2} e^{-(\cos^2\phi)\hat{t}}\,d\phi$$

$$+g\beta\tau T(0)(2/\pi)\int_0^{\pi/2}[1-e^{-(\cos^2\phi)\hat{t}}][\cos\phi]^{-2}\,d\phi. \quad (4.15)$$

We now let t become large. If we rewrite the integrals in terms of $s = \pi/2-\phi$, note that only small values of s contribute at large t, and introduce $p = s\hat{t}^{1/2}$, we find,

$$u(x,t) = \frac{1}{2\pi(\pi\hat{t})^{1/2}}\int_0^\infty e^{-k^2x^2/4\hat{t}}\cos(yk)\,U_0(k)\,k\,dk$$

$$+\frac{g\beta\tau}{\pi^2}\hat{t}^{1/2}\int_0^\infty\int_0^\infty\frac{1-e^{-p^2}}{p^2}\cos\left(\frac{xk}{\hat{t}^{1/2}}p\right)\cos(yk)\,\Gamma(k)\,k\,dk\,dp. \quad (4.16)$$

The first of the integrals has been simplified using the relationship

$$\int_0^\infty e^{-p^2}\cos(\lambda p)\,dp = (\pi^{1/2}/2)\,e^{-\lambda^2/4}; \quad \lambda = kx/\hat{t}^{1/2}.$$

The velocity on the axis at large t is particularly simple:

$$u(0,t) = \frac{u_0(0)}{(\pi\hat{t})^{1/2}}+g\beta\tau T(0)(2/\pi)(\pi\hat{t})^{1/2}. \quad (4.17)$$

Expression (4.16) confirms that, as anticipated, x scales as $(\alpha_B t)^{1/2}$. Consequently, (4.12) is indeed the correct form at large times. Notice that, for isothermal jets, elongation of the jet cross-section has produced an algebraic decay of $u(u \sim t^{-1/2})$, while buoyant jets grow continuously $(u \sim t^{1/2})$. This is entirely consistent with the arguments of §3, and contrasts with the hypothetical case where the jet cross-section does not deform and so either u decays exponentially (isotherm jets) or else saturates at $u \sim g\beta T\tau$ (buoyant jets). (See expressions (3.10) and (3.11).)

It is clear from (4.16) that the jet velocity at large times must always be of the form

$$u(x,t) = \frac{u_0(0)}{\hat{t}^{1/2}}F_1(x/\hat{t}^{1/2},y)+g\beta\tau T(0)\,\hat{t}^{1/2}F_2(x/\hat{t}^{1/2},y), \quad (4.18)$$

where F_1 is determined by the initial conditions and F_2 depends on the temperature distribution. Expression (4.18) shows a remarkably simple dependence of u on t. Moreover, it indicates that we may reduce the number of independent variables in

(4.11) from three to two. Consider, for example, an isothermal jet. Substituting (4.18) into (4.11) gives

$$\frac{\partial F_1}{\partial \chi} = \frac{\partial^2 F_1}{\partial y^2}; \quad \chi = x^2/4\hat{t}. \tag{4.19}$$

Yet again we have a diffusion equation, only this time information diffuses out along the y-axis as χ increases. Any asymptotic result we obtain from (4.16) must be a solution of (4.19).

Finally, we note that, by virtue of (4.18), the kinetic energy of the jet varies as

$$E \sim E_0/\hat{t}^{1/2}$$

for an isothermal jet, and

$$E \sim g\beta\tau T(0)\,\hat{t}^{3/2}$$

for a buoyant jet. In fact, we can find exact expressions for the global energy and dissipation integrals, E and D, using Parseval's theorem. This gives

$$E = \frac{1}{2\pi^2}\int_0^\infty \int_0^{\pi/2} U^2 k\,\mathrm{d}k\,\mathrm{d}\phi, \tag{4.20}$$

$$D = \frac{1}{\tau\pi^2}\int_0^\infty \int_0^{\pi/2} \cos^2\phi\, U^2 k\,\mathrm{d}k\,\mathrm{d}\phi. \tag{4.21}$$

For an isothermal jet, these integrals become

$$E = E_0\left(\frac{2}{\pi}\right)\int_0^{\pi/2} \mathrm{e}^{-2(\cos^2\phi)\hat{t}}\,\mathrm{d}\phi, \tag{4.22}$$

$$D = \frac{2E_0}{\tau}\left(\frac{2}{\pi}\right)\int_0^{\pi/2} \cos^2\phi\, \mathrm{e}^{-2(\cos^2\phi)\hat{t}}\,\mathrm{d}\phi. \tag{4.23}$$

Conversely, for a buoyant jet with zero initial momentum, we find

$$E = \frac{(g\beta\tau T_{rms})^2}{2}\left(\frac{2}{\pi}\right)\int_0^{\pi/2} [1-\mathrm{e}^{-(\cos^2\phi)\hat{t}}]^2 (\cos\phi)^{-4}\,\mathrm{d}\phi, \tag{4.24}$$

$$D = \frac{(g\beta\tau T_{rms})^2}{\tau}\left(\frac{2}{\pi}\right)\int_0^{\pi/2} [1-\mathrm{e}^{-(\cos^2\phi)\hat{t}}]^2 (\cos\phi)^{-2}\,\mathrm{d}\phi. \tag{4.25}$$

As before, T_{rms} is defined as the square-root of the integral of T^2. For large t, E and D take on particularly simple forms. These may be found using the same procedure that furnished (4.16). For the case of an isothermal jet, we find

$$E = \frac{E_0}{(2\pi\hat{t})^{1/2}}; \quad t \to \infty, \tag{4.26}$$

$$D = \frac{E_0/\tau}{2(2\pi)^{1/2}\,\hat{t}^{3/2}}; \quad t \to \infty, \tag{4.27}$$

while a buoyant jet with zero initial momentum behaves as

$$E = (g\beta\tau T_{rms})^2 \frac{4(\sqrt{2}-1)}{3\pi^{1/2}}\,\hat{t}^{3/2}; \quad t \to \infty, \tag{4.28}$$

$$D = \frac{(g\beta\tau T_{rms})^2}{\tau}\frac{4(\sqrt{2}-1)}{(2\pi)^{1/2}}\,\hat{t}^{1/2}; \quad t \to \infty. \tag{4.29}$$

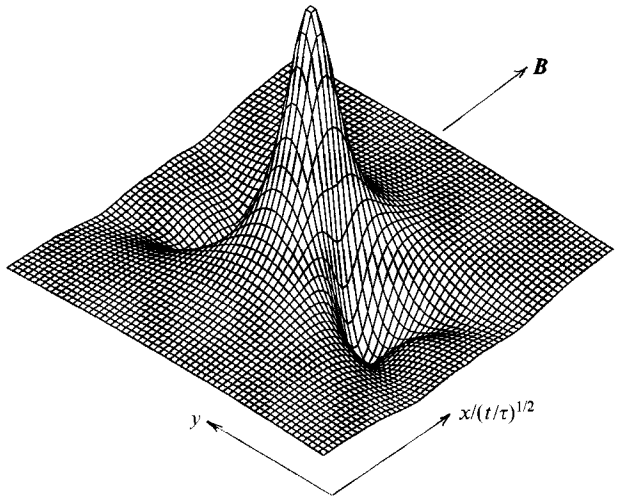

FIGURE 7. Transient damping of a jet in an infinite domain: shape of the velocity profile at large times. The x-axis has been scaled by $(t/\tau)^{1/2}$.

These expressions show the expected $t^{-1/2}$ and $t^{3/2}$ dependence for E, which is an inevitable consequence of (4.18). Note also that the relative dissipation, D/E, decreases with time, as predicted by (3.6).

We conclude this discussion of the flow structure at large times with a simple numerical example. Consider the case of an isothermal jet, with an initial velocity distribution of

$$u_0(r) = V\,\mathrm{e}^{-r^2/\delta^2}.$$

This initial condition transforms to

$$U_0(k) = \pi V\delta^2\,\mathrm{e}^{-k^2\delta^2/4}$$

and so the velocity distribution at large t is

$$u(x,t) = \frac{V\delta^2}{2(\pi\hat{t})^{1/2}}\int_0^\infty \exp\left[-\frac{k^2\delta^2}{4}\left(1+\frac{x^2}{\delta^2\hat{t}}\right)\right]\cos(yk)\,k\,\mathrm{d}k.$$

This may be integrated to give

$$u(x,t) = \frac{V}{(\pi\hat{t})^{1/2}}\frac{1}{[1+x^2/(\delta^2\hat{t})]}G(\zeta);\quad \zeta = \frac{y^2}{\delta^2+x^2/\hat{t}}, \tag{4.30}$$

where G is Kummer's hypergeometric function

$$G(\zeta) = M(1,\tfrac{1}{2},-\zeta) = M(-\tfrac{1}{2},\tfrac{1}{2},\zeta)\,\mathrm{e}^{-\zeta}.$$

The shape of this velocity distribution is shown in figure 7. As expected, the jet cross-section elongates at the rate $t^{1/2}$, while regions of reverse flow are clearly visible to either side of the central jet.

In summary then, elongation of the jet cross-section, anticipated in §3 and implied by figure 4, persists to large times, where the jet adopts a sheet-like structure with regions of reverse flow. This continual distortion of the jet minimizes the (relative) Joule dissipation, D/E, by forcing longer and longer return paths on the induced current. It also provides the essential mechanism for conserving or maintaining linear momentum. Let us now see how these ideas carry over to a jet developing in space rather than time.

5. Example 2. MHD jets formed by sidewall injection

We now turn our attention to the geometry shown in figure 1(*b*). Here a submerged jet is formed by injecting fluid through a circular aperture in a sidewall. A uniform vertical magnetic field is applied to the jet, acting to dissipate the motion. This steady flow is the three-dimensional equivalent of the two-dimensional jets of Moreau (1963*a*, *b*) and of Moffatt & Toomre (1967).

Before performing a formal analysis of this problem, let us try to construct a picture of what occurs. As the jet emerges into the $\boldsymbol{B}$-field, currents are induced in the y-direction by $\sigma \boldsymbol{u}_z \times \boldsymbol{B}$. This, in turn, produces a braking force on the jet. However, like Moffatt & Toomre, we have taken the magnetic interaction parameter, N, to be small. That is, the magnetic forces are much smaller than the jet inertia. Thus, initially, the $\boldsymbol{B}$-field has only a slight effect on the jet, and so it continues to propagate in the z-direction. The magnetic forces do ultimately influence the jet, but this is a relatively slow process, so that the characteristic length scale in the z-direction, l_z, is much greater than l_x and l_y. Thus the jet adopts a long thin shape. Now the currents $\sigma \boldsymbol{u}_z \times \boldsymbol{B}$ must form closed paths. Since each cross-section of the jet looks very much like its neighbouring cross-sections, these currents close within the (x, y)-plane, just as they did in our transient problem. The situation is as shown in figure 8. The current paths adopt the characteristic dipole-like structure, with the induced current returning through regions of weak or zero flow. It follows that a reverse flow is induced at points on the y-axis (marked R in figure 8*b*), where the Lorentz force is negative and the jet velocity is small. In addition, momentum diffuses out along the x-axis to points marked A, where the Lorentz force is positive and the jet velocity is again small. In short, for precisely the same reasons as outlined in §4, momentum diffuses out along the x-axis and the jet cross-section becomes long and elongated.

Now if the jet is to spread in the x-direction, then continuity requires that there is some entrainment of the surrounding fluid. (We shall confirm later that the mass flux in the jet does indeed increase with z.) We would expect, therefore, that the jet draws in fluid from the far field, predominantly at large $|x|$. Conversely, the region of reverse flow on the y-axis will produce an outward flow of mass near the wall. This is illustrated in figure 9. All-in-all, we expect a relatively complex, three-dimensional flow pattern.

We now devote the rest of this section to justifying the picture given above. Of course, the governing equations for this flow are complex and nonlinear, and so we cannot readily find simple analytical solutions. This is further complicated by the existence of a reverse flow, which limits the degree to which we can specify the upstream conditions. However, we shall construct general arguments which establish the essential features of the motion. In particular, we shall show that elongation of the jet cross-section is both inevitable and essential, and that reverse flow will, in general, occur. In addition, we shall establish the scaling laws for all three velocity components, and determine the rate of spreading of the jet with respect to z. The starting point for our analysis is equation (2.10), in the form

$$\nabla^2\{\boldsymbol{u}\cdot\nabla\boldsymbol{u}\}-\nabla\left\{\frac{\partial^2(u_i u_j)}{\partial x_i \partial x_j}\right\}+\frac{1}{\tau}\frac{\partial^2 \boldsymbol{u}}{\partial x^2}=0. \tag{5.1}$$

Consider the z-component of this equation. If we equate the first and last terms, and take $l_y \sim \delta$, then we can express the interaction parameter, N, in terms of l_x, l_y and l_z:

$$N \sim l_x^2/\delta l_z.$$

It follows that, as expected, the jet develops slowly when N is small, in the sense that

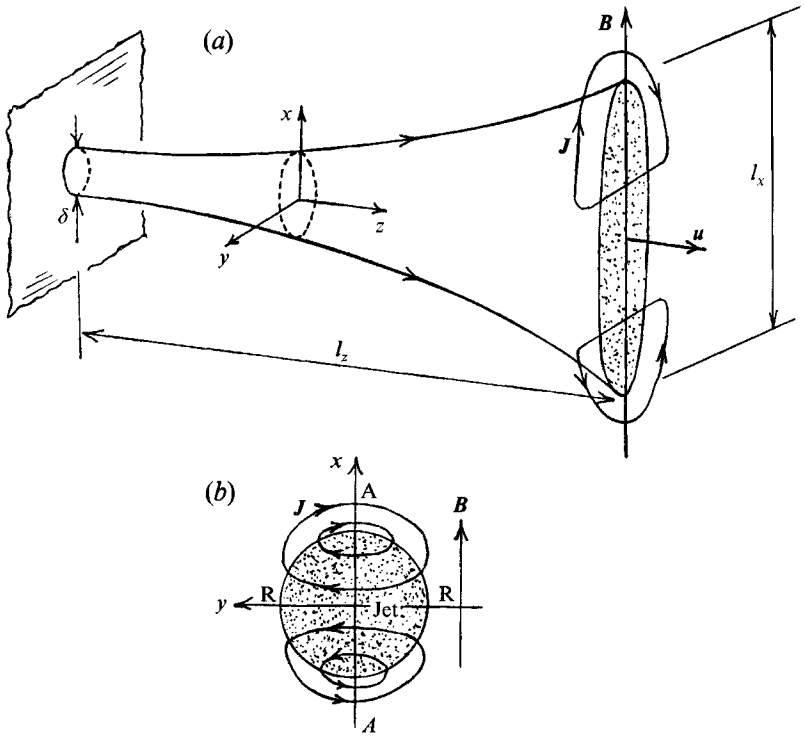

FIGURE 8. MHD jet produced by sidewall injection: (*a*) spatial evolution of the jet; and (*b*) current paths in the (x, y)-plane. Reverse flow occurs at points marked R and energy diffuses out to points marked A.

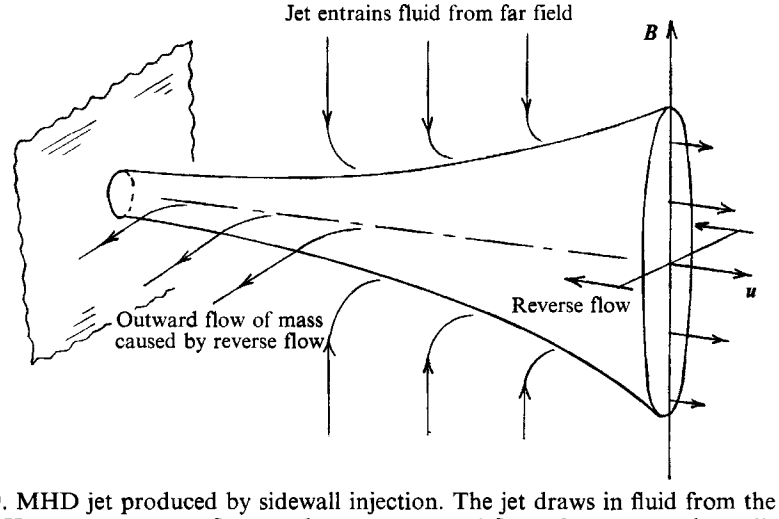

FIGURE 9. MHD jet produced by sidewall injection. The jet draws in fluid from the far field. However, a reverse flow produces an outward flow of mass near the wall.

$l_z \gg l_x, \delta$. Next, we note that the second term in (5.1) is of order u_z^2/l_z^3, which is a factor of $(\delta/l_z)^2$ smaller than the other terms. It follows that the z-component of (5.1) simplifies to

$$\nabla_{xy}^2(\boldsymbol{u}\cdot\nabla u_z) = -\frac{1}{\tau}\frac{\partial^2 u_z}{\partial x^2}. \tag{5.2}$$

This equation of motion may be rewritten in the more familiar form

$$\frac{\mathrm{D}u_z}{\mathrm{D}t} = \boldsymbol{u}\cdot\nabla u_z = -\frac{1}{\tau}\nabla_{xy}^{-2}\left[\frac{\partial^2 u_z}{\partial x^2}\right], \tag{5.3}$$

where the operator ∇_{xy}^{-2} is defined through the expression

$$\nabla_{xy}^{-2} f = \frac{1}{4\pi}\int f(x',y')\ln[(x-x')^2+(y-y')^2]\,\mathrm{d}A'.$$

Equation (5.3) might be compared with (4.5) for our transient, one-dimensional jet,

$$\frac{\partial u_z}{\partial t} = -\frac{1}{\tau}\nabla_{xy}^{-2}\left[\frac{\partial^2 u_z}{\partial x^2}\right]. \tag{5.4}$$

Clearly, as noted in §2, there is a direct analogy between the two problems, with the temporal development of one corresponding to the spatial development of the other. This correspondence allows us to establish that a region of reverse flow does indeed occur. The argument is straightforward. We already know from the examples in §4 that, for a typical jet-like distribution of u_z, the operator

$$F(u_z) = -\frac{1}{\tau}\nabla_{xy}^{-2}\left[\frac{\partial^2 u_z}{\partial x^2}\right]$$

produces negative values of F at all points on the y-axis, including those where u_z is zero or small. Now in this problem the interaction parameter is small. Consequently, the magnetic forces are weak and the initial shape of the jet is determined largely by the inlet conditions. It follows that, initially, u_z will have a typical jet-like distribution, and so F will induce a reverse flow on the y-axis. Of course, this reverse flow disrupts the initial conditions and our argument becomes somewhat circular. However, if the magnetic field is sufficiently weak ($N \ll 1$) we might expect, on physical grounds, that we can specify the velocity in the immediate vicinity of the orifice.

It is natural to enquire as to the physical origin of (5.3). This may be established as follows. Since $l_z \gg l_x$, δ and $u_z \gg u_x$, u_y, the pressure is a function of z alone (to order N^2). But the pressure is zero at large x and y, and so it follows that p is everywhere zero. The equation of motion in the z-direction is therefore

$$\boldsymbol{u}\cdot\nabla u_z = F_z.$$

It only remains to show that the right-hand side of (5.3) is indeed the Lorentz force, F_z. This arises from the two-dimensional nature of $\boldsymbol{J}$, which in turn follows from the fact that $l_z \gg l_x, \delta$ and $u_z \gg u_x, u_y$. Since $\boldsymbol{J}$ is confined to the (x,y)-plane, we may re-introduce the vector potential

$$\boldsymbol{J} = \sigma B\nabla\times(\psi\hat{\boldsymbol{e}}_z),$$

where, as before, Ohm's law requires

$$\nabla_{xy}^2\psi = -\partial u_z/\partial x. \tag{5.5}$$

The Lorentz force is then given by (4.3), and so the equation of motion is indeed

$$\boldsymbol{u}\cdot\nabla u_z = \frac{1}{\tau}\frac{\partial\psi}{\partial x} = -\frac{1}{\tau}\nabla_{xy}^{-2}\left[\frac{\partial^2 u_z}{\partial x^2}\right]. \tag{5.6}$$

We now revisit the ideas of conservation of momentum and destruction of energy, only

this time in the context of a jet evolving in space rather than time. That momentum is conserved follows directly from (5.6). In particular, at large r we have

$$\psi \rightarrow \frac{-x}{2\pi r^2}\int u_z \, \mathrm{d}A$$

so that the right-hand side of (5.6) integrates to zero. If M is the momentum flux in the jet, then

$$M = \int u_z^2 \, \mathrm{d}A = \text{const.} \tag{5.7}$$

In this sense, an MHD jet behaves just like a conventional jet, conserving momentum but, as we shall see, entraining mass. This is in marked contrast with a two-dimensional MHD jet, where momentum is destroyed. (Moffatt & Toomre 1967 noted this essential difference.)

Next, we construct an energy equation from (5.6), analogous to (4.6):

$$\boldsymbol{u}\cdot\boldsymbol{\nabla}(\tfrac{1}{2}u_z^2) = -(\sigma\rho)^{-1}\boldsymbol{J}^2 - \boldsymbol{\nabla}\cdot(\Phi\boldsymbol{J}/\rho). \tag{5.8}$$

As before, we have a flux of kinetic energy, $\Phi\boldsymbol{J}/\rho$, out along the $\boldsymbol{J}$-lines. This energy flux is directed out of the core of the jet and towards large $|x|$, and is the mechanism by which momentum diffuses out along the magnetic field lines. (See figure 5.) In integral form, (5.8) becomes

$$\frac{\mathrm{d}}{\mathrm{d}z}\int \tfrac{1}{2}u_z^3 \, \mathrm{d}A = -\frac{1}{\tau}\int (\nabla\psi)^2 \, \mathrm{d}A = -D, \tag{5.9}$$

which confirms that energy is continually dissipated as the jet propagates forward. More importantly, this global energy equation provides independent confirmation that the jet cross-section must elongate in the x-direction. The argument is as follows. First, we rewrite (5.6) in the form

$$\boldsymbol{u}\cdot\boldsymbol{\nabla}u_z + \frac{u_z}{2\tau} = -\frac{1}{2\tau}\nabla_{xy}^{-2}\left[\frac{\partial^2 u_z}{\partial x^2} - \frac{\partial^2 u_z}{\partial y^2}\right]. \tag{5.10}$$

If the jet were to remain axisymmetric, then the left-hand side of (5.10) would be zero, and so the jet would come to a halt within a finite distance ($z_{max} \sim 2\tau u_0$). This is similar to the annihilation of a two-dimensional jet. However, in our case momentum must be conserved, and so the jet cannot come to a halt. It follows that some distortion of the jet cross-section must occur in order to reduce the dissipation of energy. From (5.5) and (5.9) we have

$$\frac{\mathrm{d}}{\mathrm{d}z}\int \tfrac{1}{2}u_z^3 \, \mathrm{d}A = -D \sim -\frac{M}{\tau}\left(\frac{\delta}{l_x}\right)^2. \tag{5.11}$$

Clearly, elongation of the jet cross-section is essential to conserving momentum, providing a mechanism for lowering the dissipation.

Let us now consider the rate at which the jet spreads, and the velocity falls, with z. We may rewrite (5.11) in the form

$$\frac{\mathrm{d}}{\mathrm{d}z}[Mu_z] \sim -\frac{M}{\tau}\left(\frac{\delta}{l_x}\right)^2,$$

while (5.7) gives us

$$M \sim u_z^2 \, \delta l_x = \text{const.}$$

It follows that u_z and l_x are of order

$$u_z \sim \left\{\frac{\tau M^2}{\delta^4 z}\right\}^{1/3} \sim \left\{\frac{M^2/\delta^2}{\alpha_B z}\right\}^{1/3}, \tag{5.12}$$

$$l_x \sim \left\{\frac{\delta^5 z^2}{\tau^2 M}\right\}^{1/3} \sim \left\{\frac{\alpha_B^2 z^2}{M/\delta}\right\}^{1/3}. \tag{5.13}$$

Here, α_B is the diffusivity, δ^2/τ. Evidently, the jet cross-section spreads along the $\boldsymbol{B}$-lines at the rate of $\sim z^{2/3}$. Notice that the mass flux in the jet also increases with z:

$$Q = \int u_z \, \mathrm{d}A \sim \left(\frac{M\delta^4 z}{\tau}\right)^{1/3}. \tag{5.14}$$

Consequently, just as with a conventional viscous jet, there must be some entrainment of mass from the far-field, as shown in figure 9. Interestingly, this is precisely the opposite of a two-dimensional MHD jet, where mass flows away from the jet.

We can gain some additional insight into the nature of the flow if we focus on the symmetry plane $y = 0$. Analysis of this flow should capture the spreading of the jet cross-section as well as the decline in centreline jet velocity. For large z we have $l_x \gg \delta$, and consequently the axial equation of motion reduces to

$$\frac{\partial^2}{\partial y^2}[\boldsymbol{u} \cdot \boldsymbol{\nabla} u_z] = -\frac{1}{\tau}\frac{\partial^2 u_z}{\partial x^2}. \tag{5.15}$$

We expect the transverse lengthscale for u_z to be of order δ. In addition, u_y is zero on the x-axis, so that we may rewrite (5.15) as

$$u_x \frac{\partial u_z}{\partial x} + u_z \frac{\partial u_z}{\partial z} \sim \alpha_B(x, z)\frac{\partial^2 u_z}{\partial x^2}; \quad \alpha_B \sim \delta^2/\tau. \tag{5.16}$$

To appreciate the kinds of flows which satisfy (5.16), consider the simplest case where α_B is a constant. Then (5.26) has the well-known solution

$$u_z = \left(\frac{3M^2}{32\alpha_B z}\right)^{1/3} \operatorname{sech}^2[x(48\alpha_B^2 z^2/M)^{-1/3}], \tag{5.17}$$

where M is now evaluated on the x-axis only. Notice that u_z and l_x scale as predicted. Interestingly, if we substitute ν for α_B, (5.17) becomes the classic solution for a conventional viscous, two-dimensional jet (a sheet) emerging from a slit. As with our MHD jet, momentum in a viscous jet is conserved, the jet spreads in the x-direction, and the mass flux increases with z, so that the jet entrains fluid from large $|x|$. The case where α_B is not a constant might be thought of as corresponding to a laminar jet of variable viscosity.

We conclude this section by looking at the scaling of the other velocity components. As we have three unknowns, u_x, u_y and u_z, we require three governing equations. These are furnished by the continuity equation along with any two components of (5.1). We shall take the x- and z-components. For large z, our three governing equations are

$$\frac{\partial^2}{\partial y^2}[\boldsymbol{u} \cdot \boldsymbol{\nabla} u_z] + \frac{1}{\tau}\frac{\partial^2 u_z}{\partial x^2} = 0, \tag{5.18a}$$

$$\frac{\partial^2}{\partial y^2}[\boldsymbol{u} \cdot \boldsymbol{\nabla} u_x] + \frac{1}{\tau}\frac{\partial^2 u_x}{\partial x^2} = 0, \tag{5.18b}$$

$$\boldsymbol{\nabla} \cdot \boldsymbol{u} = 0. \tag{5.18c}$$

Based on the scalings (5.12) and (5.13), we might anticipate that the components of $\boldsymbol{u}$ take the form

$$u_z = \frac{1}{2}\left[\frac{3M^2\tau}{4\delta^4 z}\right]^{1/3} F(\chi,\zeta), \tag{5.19a}$$

$$u_x = \left[\frac{\delta M}{6\tau z^2}\right]^{1/3} G(\chi,\zeta), \tag{5.19b}$$

$$u_y = \frac{1}{6}\left[\frac{3M^2\tau}{4\delta z^4}\right]^{1/3} H(\chi,\zeta), \tag{5.19c}$$

where $$\chi = \frac{x}{2[6\delta^5 z^2/\tau^2 M]^{1/3}}; \quad \zeta = \frac{y}{\delta},$$

and F is normalized such that

$$\int\int F^2 \,\mathrm{d}\chi\,\mathrm{d}\zeta = \tfrac{4}{3}.$$

In fact, it is readily confirmed that equations (5.18) do indeed admit such a similarity solution, with the number of independent variables reduced from three to two:

$$\frac{\partial^2}{\partial\zeta^2}\left[\frac{\partial}{\partial\chi}(\chi F^2) - G\frac{\partial F}{\partial\chi} - H\frac{\partial F}{\partial\zeta}\right] = \frac{1}{2}\frac{\partial^2 F}{\partial\chi^2}, \tag{5.20a}$$

$$\frac{\partial^2}{\partial\zeta^2}\left[2F\frac{\partial}{\partial\chi}(\chi G) - G\frac{\partial G}{\partial\chi} - H\frac{\partial G}{\partial\zeta}\right] = \frac{1}{2}\frac{\partial^2 G}{\partial\chi^2}, \tag{5.20b}$$

$$\frac{\partial H}{\partial\zeta} + \frac{\partial G}{\partial\chi} = F + 2\chi\frac{\partial F}{\partial\chi}. \tag{5.20c}$$

In addition, in cases where the y-component of velocity is zero, we end up with a particularly simple (diffusion-like) equation for F,

$$\frac{\partial f}{\partial\chi} = \frac{\partial^2 f^2}{\partial\zeta^2} + F(0,\zeta); \quad f = \int_0^\chi F\,\mathrm{d}\chi. \tag{5.21}$$

This is analogous to (4.19) for our transient one-dimensional jet. However, it is doubtful that jet flows exist in which u_y is zero, particularly when there is a region of reverse flow on the y-axis. We are left then with three nonlinear equations for F, G and H, which are too complex for exact solutions to be found. Nevertheless, the fact that the governing equations do admit solutions of the form (5.19) suggests that, given the appropriate boundary conditions, these scalings are valid.

In summary, we have largely justified the picture given at the beginning of this section. There is a close relationship between the spatial development of a steady-state jet and the temporal development of its one-dimensional analogue. Reverse flow will occur on the y-axis, essentially because the operator $\nabla_{xy}^{-2}(\partial^2 u_z/\partial x^2)$ induces negative forces all along the y-axis, even in regions where u is initially small. Moreover, elongation of the jet cross-section is essential to conserving momentum. Without this stretching, an overly strong dissipation would annihilate the jet within a finite distance of its source. Consequently, the jet develops a long thin sheet-like structure, just like those discussed in §4. Finally, l_x grows at the rate $z^{2/3}$, u_z declines as $z^{-1/3}$, and the mass flux increases with z, implying that the jet entrains fluid from the far field. (Since this

paper was first submitted, new evidence has been presented which directly supports this picture. Physical and numerical experiments have been performed by Harada *et al.* (1994) of just such a flow, clearly indicating spreading of the jet along the field lines, as well as the predicted regions of reverse flow.)

Surprisingly, all of these characteristics have their counterpart in the magnetic damping of vortex flows.

6. Example 3. Damping of axisymmetric vortices

For our final example, we return to the topic of damped vortices first introduced in §3.3. This time, however, we restrict ourselves to axisymmetric flows, as this allows us to examine the interaction between damped and undamped components of motion.

Suppose we have a region of intense swirl, of characteristic radius δ, in an otherwise quiescent fluid. Let the axis of rotation be parallel to $\boldsymbol{B}$ and, for simplicity, let the flow be axisymmetric. This time we take $\boldsymbol{B}$ to point along the z-axis, as shown in figure 10. As with the jet flows we take the Reynolds number to be large and the magnetic Reynolds number to be small. However, unlike the jet flows we place no restriction on the size of the interaction parameter, N.

In general, the flow field comprises of two components: the azimuthal velocity, $\boldsymbol{u}_\theta$, and a poloidal recirculation, $\boldsymbol{u}_p$. In terms of the angular momentum Γ, and Stokes streamfunction, Ψ, we have

$$\boldsymbol{u} = \boldsymbol{u}_\theta + \boldsymbol{u}_p = (\Gamma/r)\,\hat{\boldsymbol{e}}_\theta + \nabla \times [(\Psi/r)\,\hat{\boldsymbol{e}}_\theta], \tag{6.1}$$

where

$$\nabla_*^2 \Psi = \frac{\partial^2 \Psi}{\partial z^2} + r\frac{\partial}{\partial r}\left(\frac{1}{r}\frac{\partial \Psi}{\partial r}\right) = -r\omega_\theta. \tag{6.2}$$

Since the Lorentz force is linear in $\boldsymbol{u}$, we may calculate separately the contributions of $\boldsymbol{u}_\theta$ and $\boldsymbol{u}_p$ to $\boldsymbol{F}$. Consider first the poloidal velocity. Here $\boldsymbol{\omega}_\theta \cdot \boldsymbol{B}$ is zero and so, from (2.5), the corresponding electrostatic potential is also zero. Physically, since the induced currents are azimuthal, the current paths automatically close on themselves, and so there is no requirement for a potential. It follows from (2.7) that

$$\boldsymbol{F}_p = -\frac{u_r}{\tau}\hat{\boldsymbol{e}}_r = \frac{1}{r\tau}\frac{\partial \Psi}{\partial z}\hat{\boldsymbol{e}}_r. \tag{6.3}$$

Now consider the contribution of $\boldsymbol{u}_\theta$ to $\boldsymbol{F}$. This time $\boldsymbol{J}$ is poloidal and so we may introduce a streamfunction analogous to (4.1):

$$\boldsymbol{J}_p = (\sigma B)\,\nabla \times [(\psi/r)\,\hat{\boldsymbol{e}}_\theta].$$

Ohm's law, in the form of (2.6), then requires

$$\nabla_*^2 \psi = -\partial \Gamma/\partial z \tag{6.4}$$

and so the azimuthal Lorentz force may be written as

$$rF_\theta = \frac{1}{\tau}\frac{\partial \psi}{\partial z} = -\frac{1}{\tau}\nabla_*^{-2}\left[\frac{\partial^2 \Gamma}{\partial z^2}\right]. \tag{6.5}$$

Note that this azimuthal torque disappears when the axial gradient in Γ is zero. Physically, this arises because, when $\Gamma = \Gamma(r)$, the would-be current $\sigma(\boldsymbol{u}_\theta \times \boldsymbol{B})$ points radially outwards and is independent of z. By symmetry, this current has no means of recirculating, and so $\boldsymbol{u}_\theta \times \boldsymbol{B}$ is exactly balanced by a radial gradient in the potential, Φ.

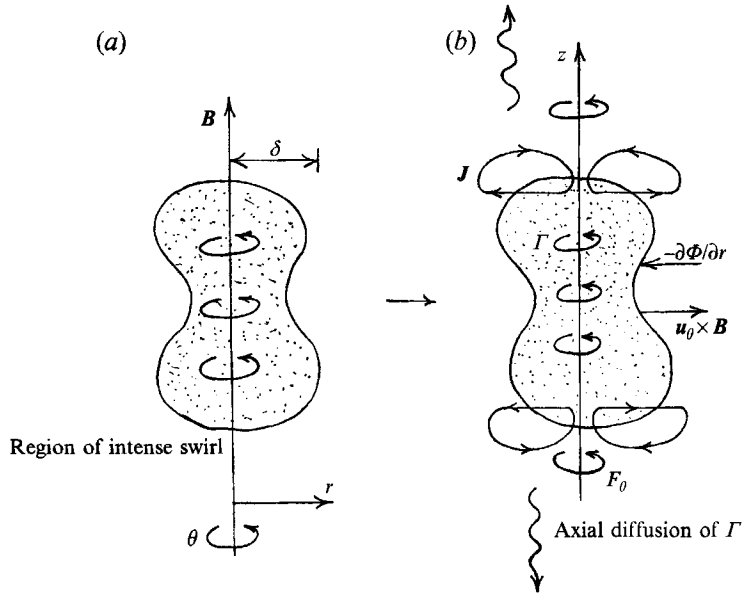

FIGURE 10. Magnetic damping of a region of intense swirl: (*a*) the initial swirl distribution; and (*b*) the axial diffusion of angular momentum.

The azimuthal and poloidal components of Euler's equation now furnishes two scalar equations. One is an equation of motion for Γ, and the other is a vorticity transport equation for ω_θ (Davidson 1993). The equation for ω_θ contains a familiar source term, which is proportional to $\partial\Gamma^2/\partial z$, and represents a corkscrewing of the poloidal vortex lines by the swirl:

$$\frac{\mathrm{D}\Gamma}{\mathrm{D}t} = \frac{1}{\tau}\frac{\partial \psi}{\partial z} = -\frac{1}{\tau}\nabla_*^{-2}\left[\frac{\partial^2 \Gamma}{\partial z^2}\right], \tag{6.6}$$

$$\frac{\mathrm{D}}{\mathrm{D}t}\left(\frac{\omega_\theta}{r}\right) = \frac{\partial}{\partial z}\left(\frac{\Gamma^2}{r^4}\right) + \frac{1}{\tau}\frac{\partial^2}{\partial z^2}\left[\frac{\Psi}{r^2}\right]. \tag{6.7}$$

The first of these equations is remarkably similar to (5.3) and (5.4), which govern the linear momentum in a jet. It tells us that global angular momentum is conserved,

$$\frac{\mathrm{d}}{\mathrm{d}t}\int_V \Gamma \,\mathrm{d}V = \frac{\mathrm{d}I_\Gamma}{\mathrm{d}t} = 0. \tag{6.8}$$

(Of course, this is a special case of the more general result established in §3.) It also tells us that, when axial gradients in Γ are small, angular momentum diffuses along the magnetic field lines, according to

$$\frac{\mathrm{D}\Gamma}{\mathrm{D}t} \sim \left(\frac{\delta^2}{\tau}\right)\frac{\partial^2 \Gamma}{\partial z^2}. \tag{6.9}$$

This is analogous to the diffusion of linear momentum in our previous examples. The mechanism of this diffusion is clear. The term $\boldsymbol{u}_\theta \times \boldsymbol{B}$ tends to drive a radial current, J_r. Near the centre of the vortex, where the axial gradient in Γ is small, this is counterbalanced by an electrostatic potential, Φ, and so no current flows. However, near the top and bottom of the vortex, the current can return through regions of small or zero swirl, as shown in figure 10(*b*). The resulting inward flow of current above and below

the vortex gives rise to a reversed azimuthal torque which, in turn, creates positive angular momentum in previously stagnant regions. Notice also that regions of reverse rotation are induced in an annular zone surrounding the initial vortex. Yet again, there is a direct analogy with the reverse flow induced by an MHD jet.

The energy equations corresponding to (6.6) and (6.7) are

$$\frac{\mathrm{d}E_\theta}{\mathrm{d}t} = -\int_V \left(\frac{u_\theta^2}{r}\right) u_r \,\mathrm{d}V - \frac{1}{\tau}\int_V \frac{(\nabla\psi)^2}{r^2}\,\mathrm{d}V, \tag{6.10}$$

$$\frac{\mathrm{d}E_p}{\mathrm{d}t} = +\int_V \left(\frac{u_\theta^2}{r}\right) u_r \,\mathrm{d}V - \frac{1}{\tau}\int_V u_r^2\,\mathrm{d}V. \tag{6.11}$$

The first term on the right of these expressions represents the familiar exchange of energy between the swirl and the poloidal motion. It arises because, whenever a region of swirl moves radially outward, conserving angular momentum, its energy, E_θ, falls. In the case of an isolated region of swirl, this exchange term represents a transfer of energy from the swirl to the recirculation as the fluid centrifuges itself radially outward (Davidson 1993). The two terms arising from the Lorentz force are, of course, negative and represent Joule dissipation.

Conservation of I_Γ, in conjuction with the energy equations (6.10) and (6.11), tells us a great deal about the evolution of our flow. In particular, if angular momentum is conserved, we can bound the kinetic energy from below using a variant of (3.15),

$$E_\theta \geqslant I_\Gamma^2 \Big/ 2\int r^2\,\mathrm{d}V. \tag{6.12}$$

The equality holds if and only if u_θ represents rigid-body rotation. On the other hand, (6.10) and (6.11) tell us that energy is continually destroyed as long as J^2 is non-zero. But J^2 is zero only when the poloidal recirculation disappears and Γ is independent of z. It follows that an arbitrary initial condition must evolve into a steady state of the form

$$\Gamma = \Gamma(r); \quad \boldsymbol{u}_p = \boldsymbol{0}.$$

The only restriction is that the initial and final angular momenta must be the same. As we shall see, the route which the flow takes to this swirl-only state depends upon the magnitude of the interaction parameter, N.

The energy equations (6.10) and (6.11) also indicate that the Lorentz force preferentially dissipates the poloidal motion. If t_p is the characteristic time scale for $\boldsymbol{u}_p$, say the turnover time ω_θ^{-1}, then (6.10) and (6.11) give us

$$\frac{\mathrm{d}E_\theta}{\mathrm{d}t} \sim \pm\frac{E_\theta}{t_p} - \frac{E_\theta}{\tau}\left(\frac{\delta}{l_z}\right)^2, \tag{6.13}$$

$$\frac{\mathrm{d}E_p}{\mathrm{d}t} \sim \mp\frac{E_\theta}{t_p} - \frac{E_p}{\tau}. \tag{6.14}$$

The Lorentz force extracts energy from the poloidal recirculation at the rate of E_p/τ. If the swirl flow does not transfer energy to E_p rapidly enough (i.e. faster than τ^{-1}), then any initial poloidal energy will decay as

$$E_p \sim E_p(0)\,\mathrm{e}^{-t/\tau}.$$

The swirl flow, on the other hand, experiences Joule dissipation at the rate of $(E_\theta/\tau)(\delta/l_z)^2$. Just as with the jet flows, the swirl can avoid destruction by stretching

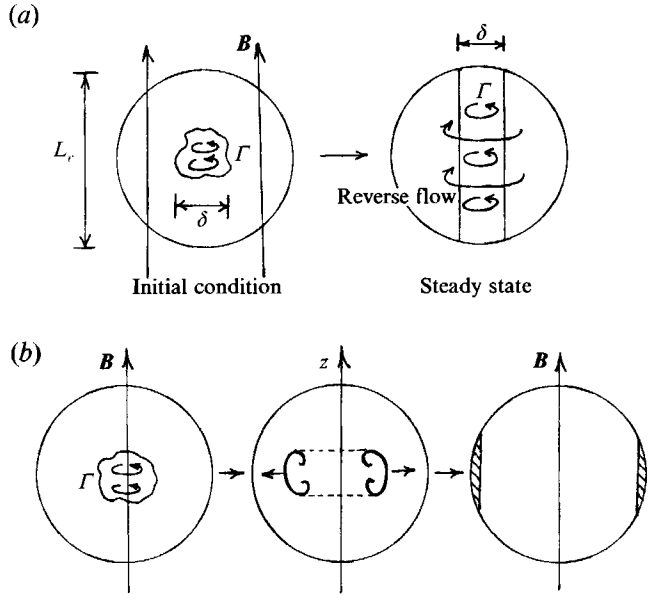

FIGURE 11. Magnetic damping of swirl: (*a*) large interaction parameter; and (*b*) small interaction parameter.

along the $\boldsymbol{B}$-lines. Indeed, it must do just this since E_θ cannot fall below the limit set by (6.12).

The picture is therefore clear. Consider first the case of a large interaction parameter, $N = t_p/\tau \gg 1$. An initial blob of swirl will induce a recirculation via the source term in (6.7). This recirculation will tend to centrifuge the angular momentum outward, so that E_θ releases energy to the poloidal velocity in accordance with (6.10) and (6.11) (Davidson 1993). This occurs on a time scale of t_p and is the beginning of a Rayleigh-like instability. However, the Lorentz force dissipates the recirculation on a time scale of τ. Since $t_p \gg \tau$, the poloidal velocity cannot grow beyond a value of $N^{-1/2}u_\theta$. In the meantime, the energy of the swirl will start to decay through Ohmic dissipation, as dictated by (6.13). However, E_θ cannot decay beyond the limit set by (6.12), and so axial diffusion of Γ must take place in order that the dissipation is reduced. Consequently, angular momentum spreads out along the z-axis, and E_θ continues to fall, until Γ reaches the boundary, S. This occurs on a time scale of $t \sim \tau(L_V/\delta)^2$, where L_V is the axial length of V. Ultimately, a steady state is reached, in which the poloidal motion is zero and Γ is a function only of r. This is illustrated in figure 11(*a*).

When the interaction parameter is small or moderate the situation is somewhat more complex. Once again, an initial blob of swirl will tend to centrifuge itself outward, releasing energy to the poloidal flow. However, this time $\tau \gg t_p$, and so the weak Lorentz forces do not inhibit the process. The angular momentum will rearrange itself into one or more rings which then propagate radially outward. (See figure 11*b*.) The cross-section of these hoops has a characteristic mushroom-like shape, reminiscent of a thermal plume rising from an impulsively heated plate (Davidson 1993). If the Lorentz force were zero, then a singularity in Γ would form at the outer edge of these rings (Pumir & Siggia 1992). However, the Joule dissipation will alleviate this to some extent, allowing Γ to diffuse. Ultimately, the angular momentum will centrifuge itself to the outer radial boundary. At this point E_θ ceases to release energy to the poloidal recirculation, since u_r falls to zero. E_p is then destroyed by the Lorentz force on a

timescale of τ, and eventually a swirl-only steady state is reached which is quite distinct from that corresponding to a large interaction parameter. (Compare figures 11*a* and 11*b*.)

In summary, then, there is a qualitative similarity between magnetic damping of swirling flow and the braking of a jet. The transport equation for angular momentum is essentially the same as that which governs the linear momentum of a jet. Just like linear momentum, angular momentum is globally conserved, and diffuses along the ***B***-lines. The fact that I_Γ is constant is particularly important, as it guarantees that each flow reaches a steady state, in which Γ is independent of z and $\boldsymbol{u}_p$ is everywhere zero.

7. Conclusions

MHD jets evolving in either space or time conserve momentum but lose energy. They achieve this by undergoing a progressive distortion of their cross-section. The jet cross-section is elongated along the magnetic field lines, developing a sheet-like structure. This lowers the Joule dissipation by forcing longer and longer return paths on the induced current. Without this distortion, an overly strong dissipation would annihilate the jet within a finite distance (or time), contravening conservation of momentum.

A similar process occurs in the magnetic damping of vortices. Here angular momentum is conserved, while the kinetic energy falls monotonically. As with the jet flows, the Lorentz force cannot destroy the vortex. Rather, it rearranges the angular momentum so as to reduce the global kinetic energy. This process ceases, and a steady state is reached, only when the angular momentum is uniform along the ***B***-lines.

These two examples illustrate the four general principles which control many forms of magnetic damping. These are:

(i) the Lorentz force destroys kinetic energy but does not alter the net linear and angular momentum of the fluid;

(ii) the Lorentz force tends to direct the flow in such a way that the relative dissipation, D/E, continually fall;

(iii) the reduction in relative dissipation, D/E, is achieved by elongating the flow along the ***B***-lines;

(iv) the spreading of momentum and vorticity along the field lines is essentially a diffusive process, with a diffusivity of δ^2/τ.

This last point is familiar in the context of MHD turbulence.

REFERENCES

ALEMANY, A., MOREAU, R., SULEM, P. L. & FRISCH, U. 1979 Influence of external magnetic field on homogeneous MHD turbulence. *J. Méc* **18**, 280–313.

ALBOUSSIERE, T., GARANDET, J. P. & MOREAU, R. 1993 Buoyancy-driven convection with a uniform magnetic field. Part 1. Asymptotic analysis. *J. Fluid Mech.* **253**, 545–563.

BANSAL, J. L. & GUPTA, M. L. 1978 Hydromagnetic laminar and turbulent free jet. *Appl. Sci. Res.* **34**, 367–379.

DAVIDSON, P. A. 1993 Similarities in the structure of swirling and buoyancy-driven flows. *J. Fluid Mech.* **252**, 357–382.

DAVIDSON, P. A. & FLOOD, S. C. 1994 Natural convection in an aluminium ingot: a mathematical model. *Metall. Mater. Trans.* B **25**, 293–301.

HARADA, H., OKAZAWA, K., TANAKA, M. & TAKEUCHI, E. 1994 The MHD counterflow around a jet from a nozzle under a DC magnetic field. *Proc. Intl. Symp. on Electromagnetic Processing of Materials, Nagoya, Japan, October 1994.* Iron & Steel Institute of Japan.

JACKSON, J. D. 1962 *Classical Electrodynamics*. John Wiley & Sons.

LIELAUSIS, O. 1975 *Atomic Energy Rev.* **13**, 527.

MOFFATT, H. K. 1967 On the suppression of turbulence by a uniform magnetic field. *J. Fluid Mech.* **28**, 571–592.

MOFFATT, H. K. & TOOMRE, J. 1967 The annihilation of a two-dimensional jet by a transverse magnetic field. *J. Fluid Mech.* **30**, 65–82.

MOREAU, R. 1963*a* Jet libre plan, laminaire, d'un fluide incompressible en presence d'un champ magnetique transversal. *C. R. Acad. Sci. Paris* **256**, 2294–2298.

MOREAU, R. 1963*b* Jet libre plan, laminaire, d'un fluide incompressible en presence d'un champ magnetique transversal. *C. R. Acad. Sci. Paris* **256**, 4849–4853.

MOREAU, R. 1990 *Magnetohydrodynamics*. Kluwer.

MULLER, G., NEUMANN, G. & WEBER, W. 1984 Natural convection in vertical Bridgman configurations. *J. Cryst. Growth* **70**, 78–93.

NAKAMURA, S., HIBIY, T., YOKOTA, T. & YAMAMOTO, F. 1990 Thermal conductivity measurements of mercury in a magnetic field. *Intl J. Heat Mass Transfer* **33**, 2609–2613.

OUGHTON, S., PRIEST, E. R. & MATTHAEUS, W. H. 1994 The influence of a mean magnetic field on three-dimensional MDH turbulence. *J. Fluid Mech.* **280**, 95–117.

PUMIR, A. & SIGGIA, E. D. 1992 Development of singular solutions of the axisymmetric Euler equations. *Phys. Fluids* A **4**, 1472–1491.

ROBERTS, P. H. 1967 *An Introduction to Magnetohydrodynamics*. Longmans.

SAITO, A., MATSUMOTO, K. & UTAKA, Y. 1987 Reconsideration of the transient line heat source technique. *JSME Intl J.* **30**, 1935–1942.

SOMMERIA, J. & MOREAU, R. 1982 Why, how, and when, MHD turbulence because two-dimensional. *J. Fluid Mech.* **118**, 507–518.

SZEKELY, J., EVANS, J. W., BLAZEK, K. & EL-KADDAH, N. 1992 *Magnetohydrodynamics in Process Metallurgy*. The Minerals, Metals and Materials Soc. of USA.